Chem. Res. Toxicol. **2009,** *22,* 1588–1593

Isolation and Identification of a Novel Aromatic Amine Mutagen Produced by the Maillard Reaction

Rena Nishigaki,[†] Tetsushi Watanabe,*[,‡] Tetsuya Kajimoto,[§] Atsuko Tada,[†] Takeji Takamura-Enya,[†] Shigeki Enomoto,[†] Haruo Nukaya,[∥] Yoshiyasu Terao,[∥] Atsushi Muroyama,[§] Minoru Ozeki,[§] Manabu Node,[§] Tomohiro Hasei,[‡] Yukari Totsuka,[†] and Keiji Wakabayashi[†]

Cancer Prevention Basic Research Project, National Cancer Center Research Institute, 1-1 Tsukiji 5-chome, Chuo-ku, Tokyo 104-0045, Japan, Department of Public Health and Department of Pharmaceutical Manufacturing Chemistry, Kyoto Pharmaceutical University, 1 Shichono-cho, Misasagi, Yamashina-ku, Kyoto 607-8412, Japan, and Graduate School of Nutritional and Environmental Sciences, University of Shizuoka, 52-1, Yada, Suruga-ku, Shizuoka 422-8526, Japan

Received March 30, 2009

To clarify the formation of mutagens in the Maillard reaction of glucose and amino acids, 20 amino acids were separately incubated with glucose in the presence or absence of hydroxyl radicals produced by the Fenton reaction. After 1 week at 37 °C and pH 7.4, the reaction mixtures of glucose and tryptophan with and without the Fenton reagent showed mutagenicity toward *Salmonella typhimurium* YG1024 in the presence of a mammalian metabolic system (S9 mix). To identify mutagens in the reaction mixture, blue rayon-adsorbed material from a mixture of glucose, tryptophan, and the Fenton reagent was separated by column chromatography using various solid and mobile phases, and one mutagen, which accounted for 18% of the total mutagenicity of the reaction mixture, was isolated. The chemical structure of the mutagen was determined to be 5-amino-6-hydroxy-8*H*-benzo[6,7]azepino[5,4,3-*de*]quinolin-7-one (ABAQ) on the basis of ESI mass, high-resolution APCI mass, ^{1}H NMR, ^{13}C NMR, and IR spectral analyses and chemical synthesis of the mutagen. The novel aromatic amine showed high mutagenicity toward *S. typhimurium* TA98 and YG1024 with S9 mix, inducing 857 revertants of TA98 and 6007 revertants of YG1024/μg, respectively. The mutagenicity of ABAQ was comparable to that of 2-amino-1-methyl-6-phenylimidazo[4,5-*b*]pyridine, which is a mutagenic and carcinogenic hetrocyclic amine in cooked meat and fish formed through the Maillard reaction at high temperature.

Introduction

The Maillard reaction is a nonenzymatic chemical reaction between reducing sugars and amino groups to form Schiff base adducts, which rearrange to form Amadori products. In the advanced Maillard reaction, the Amadori products are degraded into reactive carbonyl species, such as deoxyglucosone and methylglyoxal, and react again with free amino groups to form chromophores, fluorophores, and so forth. The Maillard reaction in vivo has been implicated in the aging process and various diseases, including diabetes, cataracts, retinopathy, and nephropathy (*1*−*3*). Elevated tissue concentrations of reactive carbonyl species are observed under pathological conditions (*4*−*6*). Pyrraline, that is, 2-amino-6-(2-formyl-5-hydroxymethylpyrrol-1-yl)hexanoic acid, is formed via the Maillard reaction between glucose and the ε-amino group of lysine (*7*) and is thought to induce biological responses, including mutations (*8, 9*). Increased levels of pyrraline were found in plasma and urine from diabetic individuals and were also detected in the sclerosed matrix of glomeruli affected by diabetic nephropathy (*10*−*14*). Many epidemiological studies have indicated positive links between diabetes and cancer of the liver, pancreas, and others (*15*−*17*). These findings suggest that mutagenic/carcinogenic compounds, such as some reactive carbonyl species and pyrraline, are formed by the Maillard reaction in vivo and increase the risk of cancer in persons with a history of diabetes. However, little is known about the chemical structure of most mutagens formed through the Maillard reaction in vivo.

In the present study, model reactions in vitro were used to find mutagens potentially produced by the Maillard reaction in vivo. Mixtures of glucose and L-amino acids were incubated at 37 °C and pH 7.4 in the presence or absence of hydroxyl radicals produced by the Fenton reaction, because hydroxyl radicals are commonly generated in vivo, for example, during inflammation (*18, 19*). The mutagenicity of the reaction mixtures was examined with the *Salmonella* assay. The mixtures of glucose and tryptophan with and without the Fenton reagent showed obvious mutagenicity. Consequently, the mixture of glucose, tryptophan, and the Fenton reagent was separated using blue rayon and column chromatography, and one mutagenic compound was isolated. The mutagen was determined to be a novel compound, a benzoazepinoqunolinone derivative, on the basis of the consistency of spectral data and chromatographic behaviors of the mutagen and the synthesized compound.

Experimental Procedures

Chemicals. Blue rayon was purchased from Funakoshi Co. Ltd. (Tokyo, Japan). L-Form of amino acids, HPLC-grade acetonitrile,

* To whom correspondence should be addressed. Tel: +81-75-595-4650. Fax: +81-75-595-4769. E-mail: watanabe@mb.kyoto-phu.ac.jp.
[†] National Cancer Center Research Institute.
[‡] Department of Public Health, Kyoto Pharmaceutical University.
[§] Department of Pharmaceutical Manufacturing Chemistry, Kyoto Pharmaceutical University.
[∥] University of Shizuoka.

10.1021/tx900119j CCC: $40.75
Published on Web 08/17/2009

Scheme 1. Chemical Synthesis of ABAQ 1[a]

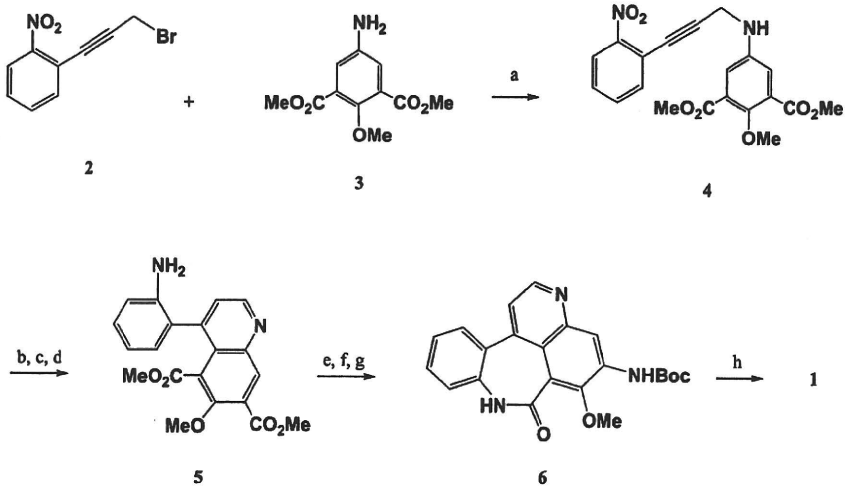

2 3 4 5 6

[a] Key: a, K_2CO_3; b, ICl, $NaHCO_3$; c, $Pd(PPh_3)_4$, HCO_2H; d, Pd-C/H_2; e, MsOH, *o*-dichlorobenzene; f, KOH aq; g, DPPA, *t*-BuOH; and h, BBr_3.

and methanol were purchased from Wako Pure Chemical Industries Co. Ltd. (Osaka, Japan). All other chemicals used were of guaranteed grade.

Reaction of Glucose and Amino Acids with or without the Fenton Reagent for Mutagenicity Assays. Glucose (0.25 mmol) and the amino acid (0.5 mmol of alanine, arginine, asparagine, aspartic acid, cysteine, glutamine, glutamic acid, glycine, histidine, isoleucine, leucine, lysine, methionine, phenylalanine, proline, serine, threonine, tryptophan, tyrosine, or valine) were dissolved in 0.5 M phosphate buffer (pH 7.4, 10 mL) with or without the Fenton reagent, that is, $FeSO_4$ (0.05 mmol) and 30% H_2O_2 (0.2 mL). Each solution was incubated at 37 °C for 1 or 3 weeks. All test samples were evaporated dry and dissolved in 50% dimethyl sulfoxide (DMSO,[1] 0.1 mL) for the mutagenicity assay.

Isolation of a Mutagen from the Reaction Mixture of Glucose and Tryptophan with the Fenton Reagent. Glucose (12.5 mmol), tryptophan (25 mmol), and $FeSO_4$ (2.5 mmol) were dissolved in 0.5 M phosphate buffer (pH 7.4, 500 mL), and 30% H_2O_2 (10 mL) was added to the solution. Then, the mixture was incubated at 37 °C for 1 week. The solution was diluted with 1.5 L of distilled water and treated with blue rayon (5 g) two times. The blue rayon was washed away with water, and adsorbed materials were extracted with 800 mL of methanol:ammonia−water (50:1, v/v) solution two times, as reported (*20*). The extract was evaporated dry. Part of the residue was used for the mutagenicity assay. The rest was further purified by column chromatography. An aliquot of each fraction obtained by column chromatography was tested for mutagenicity. The mutagenicity of the blue rayon extract and the eluate from columns were examined in *Salmonella typhimurium* YG1024 in the presence of S9 mix.

The blue rayon extract was applied to a Sephadex LH-20 column (35 mm × 860 mm, GE Healthcare UK Ltd., Buckinghamshire, England) and eluted with methanol. The first fraction was eluted with 280 mL. Thereafter, each fraction was eluted with a volume of 50 mL. Major mutagenic activity was observed in the fractions eluted at 1580−1680 mL. These mutagenic fractions were collected, evaporated, and then dissolved in methanol. The material was applied to an analytical grade YMC-Pack ODS-A 303 column (5 μm particle size, 4.6 mm × 250 mm, YMC Co. Ltd., Kyoto, Japan) for HPLC with a mobile phase of 30% acetonitrile in 25 mM phosphate buffer (pH 7.4) at a flow rate of 1 mL/min. Mutagenic fractions with retention times of 25−27 min were further purified on a CAPCELL PAK C18 ODS column (5 μm particle size, 4.6 mm × 250 mm, Shiseido Co. Ltd., Tokyo). By eluting the materials with 25% acetonitrile in 25 mM Tris-HCl buffer (pH 7.4) at a flow rate of 1 mL/min, two mutagenic fractions with retention times of 25−25.5 and 30.5−33 min were observed. The purity of the mutagenic compound (compound I) in the fractions with retention times of 30.5−33 min was confirmed on a second YMC-Pack ODS-A 303 column with a mobile phase of 30% acetonitrile in 25 mM phosphate buffer (pH 7.4) at a flow rate of 1 mL/min. The elutes were monitored for absorbance at 260 nm.

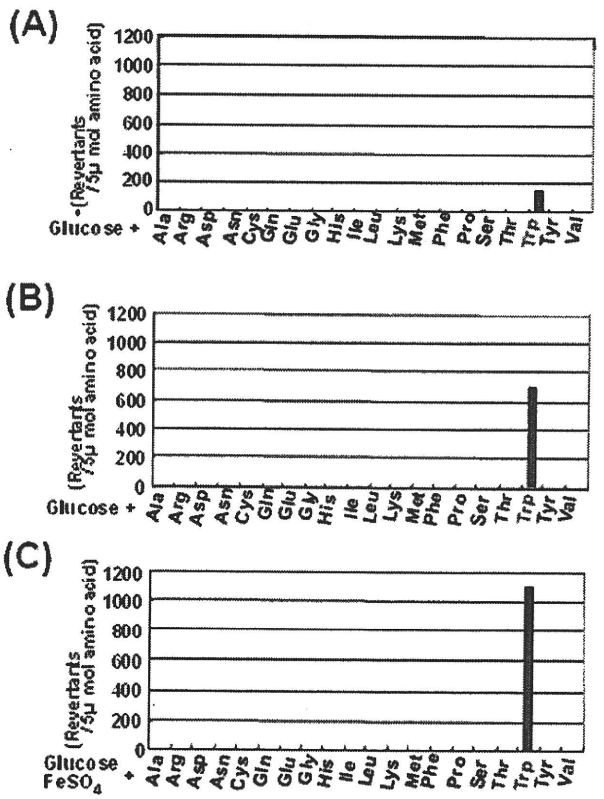

Figure 1. Mutagenicity of incubation mixtures of glucose and amino acids with or without the Fenton reagent toward *S. typhimurium* YG1024 in the presence of the S9 mix. (A) Incubation of a mixture of glucose and amino acid for 1 week, (B) incubation of a mixture of glucose and amino acid for 3 weeks, and (C) incubation of a mixture of glucose, amino acid, and the Fenton reagent for 1 week.

[1] Abbreviations: ABAQ, 5-amino-6-hydroxy-8*H*-benzo[6,7]azepino[5,4,3-*de*]quinolin-7-one; DMSO, dimethyl sulfoxide; MeIQx, 2-amino-3,8-dimethylimidazo[4,5-*f*]quinoxaline; PhIP, 2-amino-1-methyl-6-phenylimidazo[4,5-*b*]pyridine.

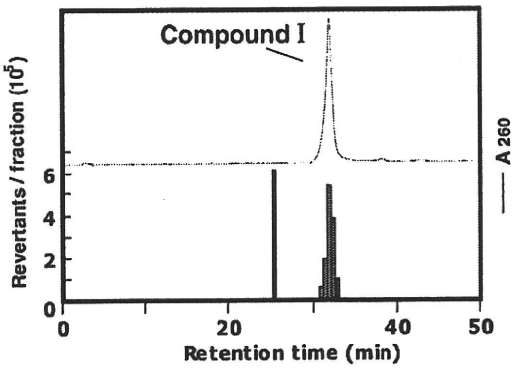

Figure 2. Purification of mutagenic compound I by HPLC. Mutagenic fractions from a YMC-Pack ODS-A 303 column with retention times of 25−27 min were purified on a CAPCELL PAK C18 ODS column. Compound I was obtained at a retention time of 32 min. The UV absorbance and mutagenicity are shown by the upper line and lower bars, respectively.

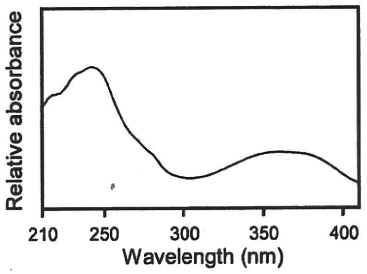

Figure 3. UV absorption spectrum of compound I, measured on the second YMC-Pack ODS-A 303 column with a photodiode array detector. The material was eluted with 30% acetonitrile in 25 mM phosphate buffer (pH 7.4).

Preparation of a Large Quantity of Compound I. In our preliminary experiment, incubation of the mixture of glucose, tryptophan, $FeSO_4$, and 30% H_2O_2 at 60 °C for 2 days with shaking enhanced the formation of compound I by about 12-fold, as compared with incubation at 37 °C for 1 week (data not shown). Glucose (62.5 mmol), tryptophan (125 mmol), and $FeSO_4$ (12.5 mmol) were dissolved in 2.5 L of 0.5 M phosphate buffer (pH 7.4), and 30% H_2O_2 (50 mL) was added to the solution. The resulting mixture was incubated at 60 °C for 2 days with shaking. In total, 90 L of mixture was incubated. Compound I in the reaction mixture was extracted with an equal amount of chloroform. The extract was then evaporated dry, and the residue was dissolved in 20 mL of methanol, filtered through a glass filter, and applied to a Sephadex LH-20 column (50 mm × 700 mm). The materials were first eluted with 460 mL of methanol, and then, methanol fractions of 40 mL were collected. The fractions at elution volumes of 2500−2820 mL, which were found to contain compound I, were combined and evaporated. The residue was dissolved in 5 mL of methanol and applied again to a Sephadex LH-20 column (30 mm × 320 mm) with methanol as a mobile phase, and fractions of 5 mL were collected after the elution of 300 mL of methanol. The fractions containing compound I, which eluted at 650−665 mL, were combined and evaporated. The residue was further purified by HPLC on a semipreparative ODS-AM 324 column (5 μm particle size, 10 mm × 300 mm, YMC Co. Ltd., Kyoto) with a mobile phase of 70% methanol at a flow rate of 2 mL/min, followed by a TSKgel CN-80Ts column (5 μm particle size, 4.6 mm × 250 mm, Tosoh Corp., Tokyo) with a mobile phase of 65% of methanol at a flow rate of 0.5 mL/min. Compound I, found in the peak fractions with retention times of 19 and 16 min on the ODS-AM 324 column and the TSKgel CN-80Ts column, respectively, was finally purified on a SUMICHIRAL OA-7100 column (5 μm particle size, 4.6 mm × 250 mm, SCAS Co. Ltd., Osaka) with a mobile phase of 50% of acetonitrile in 0.1% diethylamine−acetic acid (pH 7.4) at a flow rate of 0.5 mL/min. Compound I was isolated in the peak fraction with a retention time of 18 min. The above processes were repeated several times, and 330 μg of compound I was obtained.

Table 1. Assignments of Signals in the ^1H and ^{13}C NMR Spectra of Compound I in DMSO-d_6[a]

position	^{13}C NMR	^1H NMR
1	117.8	7.29 (1H, d, J = 4.6 Hz)
2	147.3	8.50 (1H, d, J = 4.6 Hz)
3		
3a	144.9	
4	111.9	7.20 (1H, s)
5	141.4	
6	157.4	
6a	104.5	
6b	120.3	
7	176.0	
8		10.38 (1H, s, −NH)
8a	137.0	
9	120.7	7.28 (1H, dd, J = 1.4, 7.8 Hz)
10	130.1	7.40 (1H, dt, J = 1.4, 7.8 Hz)
11	125.5	7.23 (1H, dt, J = 1.4, 7.8 Hz)
12	131.6	7.42 (1H, dd, J = 1.4, 7.8 Hz)
12a	127.7	
12b	140.6	
5-NH_2		5.78 (2H, s)

[a] Chemical shifts are expressed as ppm. s, singlet; d, doublet; dd, doublet of doublets; and dt, triplet of doublets.

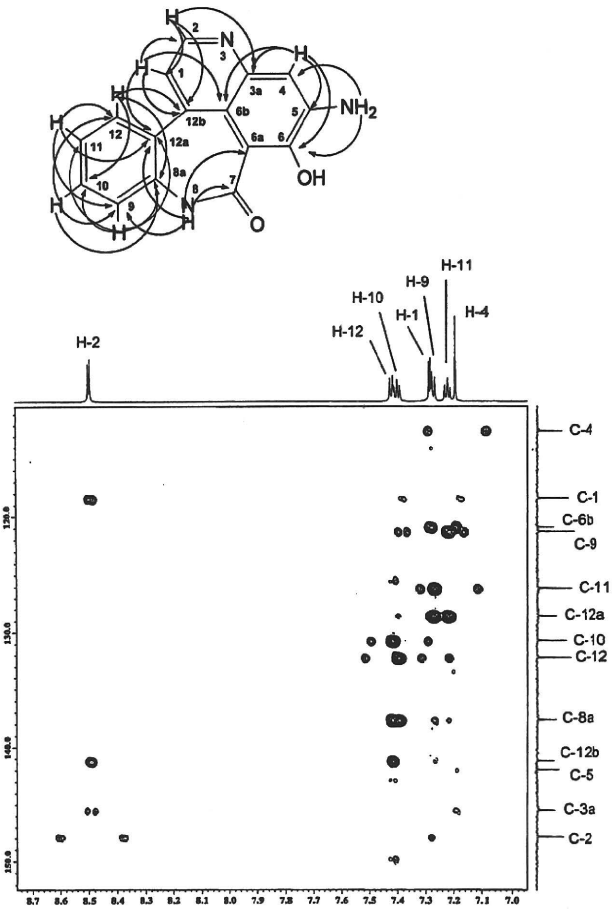

Figure 4. HMBC spectrum of compound I in DMSO-d_6.

The presence of a peak corresponding to authentic compound I was confirmed by HPLC on an analytical YMC-Pack ODS-A 303 column with a mobile phase of 30% acetonitrile in 25 mM phosphate buffer (pH 7.4) as described above.

Spectral Measurement of Compound I. ^1H NMR and ^{13}C NMR spectra were recorded with a JEOLGX-α600 or α800 instrument using microprobe FT-NMR spectrometers. The IR spectrum of

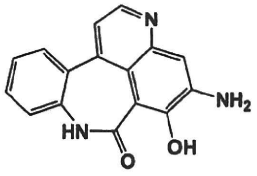

Figure 5. Chemical structure of ABAQ.

microattenuated total reflection Fourier transform infrared spectroscopy was recorded with NEXUS670 and Nic-Plan with nitrogen. High-resolution mass spectrometry was performed using an API QSTAR Pulsar i equipped with a Micro-Tech HPLC system. UV absorption spectra were measured with a Tosoh PD-8020 photodiode array detector.

Chemical Synthesis of 5-Amino-6-hydroxy-8*H*-benzo[6,7]-azepino[5,4,3-*de*]quinolin-7-one (ABAQ) 1. 1-(3-Bromoprop-1-ynyl)-2-nitrobenzene **2** was coupled with 5-amino-2-methoxyisophthalic acid dimethyl ester **3** in the presence of potassium carbonate to afford 2-methoxy-5-[3-(2-nitrophenyl)prop-2-ynylamino]isophthalic acid dimethyl ester **4**. The coupled compound **4** was transformed to a quinoline derivative, 4-(2-aminophenyl)-6-methoxyquinoline-5,7-dicarboxylic acid dimethyl ester **5**, by using Larock's method (*21*), followed by reduction with formic acid in the presence of $Pd(PPh_3)_4$ and subsequent catalytic hydrogenation. Treatment of the quinoline derivative **5** with methanesulfuric acid provided the lactam, the methyl ester of which was saponified to carboxylic acid and further converted to *t*-butyl carbamate by Curtius rearrangement (*22*). Synchronous cleavage of the methyl ether and the *t*-Boc group in 5-*tert*-butoxycarbonylamino-6-methoxy-8*H*-benzo[6,7]azepino[5,4,3-*de*]quinolin-7-one **6** with boron tribromide furnished ABAQ **1** (Scheme 1). Details of the preparation as well as physical properties of ABAQ and synthetic intermediates are reported elsewhere (*23*). The purity of ABAQ was above 99% on HPLC.

Mutagenicity Assay. Mutagenicity was examined by the preincubation method (*24*) using *S. typhimurum* TA98 (*25*), TA100 (*25*), YG1024 (*26*), and YG1029 (*26*) in the presence and absence of S9 mix. Samples were dissolved in DMSO, unless stated otherwise. The S9 mix contained 0.05 mL of S9 in a total volume of 0.5 mL. S9 was prepared from the liver of male Sprague–Dawley rats treated with phenobarital and β-naphtoflavone in combination.

Results

Mutagenicity of the Mixtures of Glucose and Amino Acid with or without the Fenton Reagent. Figure 1 shows the mutagenicity of mixtures of glucose and amino acids with or without the Fenton reagent toward *S. typhimurium* YG1024 in the presence of S9 mix. When the mixtures were incubated for 1 week without the Fenton reagent, only the combination of glucose and tryptophan showed mutagenicity, producing 140 revertants per 5 μmol of amino acid (Figure 1A). When the mixtures were incubated for 3 weeks, again, mutagenicity was observed only with glucose and tryptophan: 700 revertants per 5 μmol of amino acid (Figure 1B), about 5 times the level after 1 week. When the Fenton reagent was incubated with the mixtures for 1 week, glucose and tryptophan showed strong mutagenicity (Figure 1C), generating 1100 revertants per 5 μmol of amino acid, which was about eight times that after 1 week of incubation without the reagent. No mutagenicity was detected in any incubation sample without S9 mix. Solutions of each component above, that is, glucose, amino acid, or the Fenton reagent and a mixture of glucose and the Fenton reagent, which were not incubated, were not mutagenic (data not shown).

Isolation of a Mutagen from the Mixture of Glucose, Tryptophan, and the Fenton Reagent. To extract mutagens from the reaction mixture of glucose, typtophan, and the Fenton reagent, blue rayon was used. The blue rayon extract showed

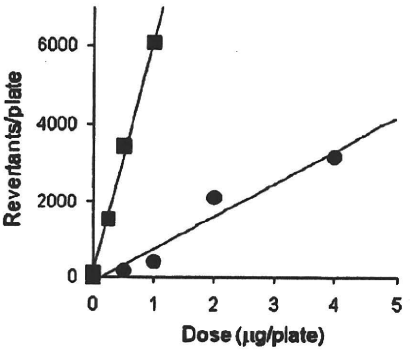

Figure 6. Mutagenicity of ABAQ toward *S. typhimurium* TA98 (●) and YG1024 (■) in the presence of S9 mix.

mutagenicity toward *S. typhimurium* YG1024 with S9 mix, its activity accounting for 72% of the mutagenicity of the mixture. By column chromatography using Sephadex LH-20, the mutagens extracted from the blue rayon were separated into four major mutagenic fractions, fractions 13–17, fractions 19–20, fractions 22–23, and fractions 26–28, which accounted for 18, 7, 14, and 26% of the total mutagenicity of the mixture, respectively. Materials in fractions 26–28 were separated by HPLC on an analytical YMC-Pack ODS-A 303 column, and the major mutagenic fraction was observed at a retention time of 25–27 min. The mutagens in this fraction were further purified by HPLC on a CAPCELL PAK C18 ODS column. Mutagenicity was mainly recovered in the two fractions with retention times of 25–25.5 and 30.5–33 min as shown in Figure 2. These fractions accounted for 7 and 18% of the mutagenicity of the mixture, respectively. In the latter fraction (retention time of 30.5–33 min), a single UV absorption peak was observed at the same retention time. On the second YMC-Pack ODS-A 303 column, the mutagenicity of the latter fraction was confirmed to be due to a single peak, and the material was designated compound I. Three micrograms of compound I was obtained from 0.5 mmol of tryptophan and 0.25 mmol of glucose in the presence of the Fenton reagent.

The UV absorption spectrum of compound I, obtained on the second YMC-Pack ODS-A 303 column with a photodiode array detector, is shown in Figure 3. Absorption maxima were found at 242 and 360 nm. With compound I isolated from the mixture described above as a marker, a large quantity of the compound was isolated from a total of 90 L of incubation mixture by column chromatography using Sephadex LH-20 and HPLC. This process was repeated several times, and 330 μg of the compound was obtained and used for various spectral analyses. The mutagenicity of compound I toward YG1024 with S9 mix was 6000 revertants/μg.

Structural Analysis of Compound I. The IR spectrum of compound I showed absorption peaks at 1641 and 1594 cm^{-1}, which suggested that an amide bond exists in the molecule, as well as a peak at 3500–3000 cm^{-1}, which suggested the presence of hydroxyl or amino groups. The mass spectrum of compound I exhibited two ion peaks, $[M + H]^+$ at *m/z* 278 in the positive mode of ESI and $[M - H]^-$ at *m/z* 276 in the negative mode. Subsequent high-resolution mass spectrometry with APCI in the negative mode indicated the molecular formula of $[M - H]^-$ to be $C_{16}H_{10}N_3O_2$ (276.0781; calculated, 276.0773). Table 1 lists chemical shifts of the proton and carbon signals in the ^1H NMR and ^{13}C NMR spectra of compound I. The ^{13}C NMR spectrum showed 16 signals only in the sp^2 carbons region. On the basis of the high-resolution mass spectrum and ^{13}C NMR spectrum, the molecular formula of compound I was confirmed to be $C_{16}H_{11}N_3O_2$. Among the 16 signals in the ^{13}C

suggest that ABAQ needs metabolism by cytochrome P450 and *O*-acetyltransferase to show mutagenicity. These characteristics were very similar to those of food-derived heterocyclic amines, reported to be formed through the Maillard reaction. The mutagenic potency of ABAQ, 857 revertants of TA98/μg and 6007 revertants of YG1024/μg, are comparable to those of PhIP, which is a mutagenic and carcinogenic heterocyclic amine (*31*).

It is possible that there might be several routes for the formation of ABAQ from glucose and tryptophan by the Maillard reaction. Scheme 2 shows one of the plausible mechanisms for the formation of ABAQ **1** from glucose and tryptophan by the Maillard reaction. First, the primary amino group of tryptophan and the aldehyde at the C-1 position of glucose were condensed to form the Schiff base **7**, the primary alcohol of which would be oxidized in the Maillard medium to carboxylic acid to afford the intermediate **8**. Next, the *ene*-reaction involving the terminal olefin of the indole, allylic proton at the β-carbon of tryptophan, and imine gave a tricyclic intermediate **9**, which was immediately converted to ε-lactam **10** accompanying deprotonation and the cleavage of a carbon−nitrogen bond. A subsequent SN2 reaction of the α-hydroxyl group of the lactam with enamine nucleophile yielded a tetracyclic compound **11** that has the basic skeleton of **1**. Decarboxylation of **11** could induce dehydration to provide the allylic alcohol **12**, which would be easily oxidized to give the α,β-unsaturated ketone **13**. The reaction of **13** with ammonium ion in the Maillard medium would form an imine intermediate **14**. Spontaneous dehydration of **14** driven by aromatic stability should furnish **1**.

In the present study, we found that a novel mutagen, ABAQ, was formed by the Maillard reaction of glucose and tryptophan in the presence and absence of hydroxyl radicals produced by the Fenton reaction. A consistent increase in blood sugar levels is a feature of diabetes, and the reaction of glucose and amino acids is thought to be enhanced in diabetic individuals. These facts suggest that ABAQ might be formed as an endogenous mutagen/carcinogen in diabetics and a population with high blood sugar levels. Further studies on the biological activities of ABAQ, such as genotocixity in vivo, and the quantification of ABAQ in biological samples from diabetic individuals are important to estimate the risk posed by ABAQ.

Acknowledgment. This study was supported by Grants-in-aid for Cancer Research from the Ministry of Health, Labor and Welfare of Japan and Scientific Research from the Ministry of Education, Culture, Sports, Science, and Technology of Japan.

References

(1) Aronson, D. (2004) Pharmacological prevention of cardiovascular aging-Targeting the Maillard reaction. *Br. J. Pharmacol. 142*, 1055–1058.

(2) Nagaraj, R. H., Shipanova, I. N., and Faust, F. M. (1996) Protein cross-linking by the Maillard reaction. Isolation, characterization, and in vivo detection of a lysine-lysine cross-link derived from methylglyoxal. *J. Biol. Chem. 271*, 19338–19345.

(3) McCance, D. R., Dyer, D. G., Dunn, J. A., Bailie, K. E., Thorpe, S. R., Baynes, J. W., and Lyons, T. J. (1993) Maillard reaction products and their relation to complications in insulin-dependent diabetes mellitus. *J. Clin. Invest. 91*, 2470–2478.

(4) Thornalley, P. J. (1994) Methylglyoxal, glyoxalases and the development of diabetic complications. *Amino Acids 6*, 15–23.

(5) Niwa, T., Takeda, N., Miyazaki, T., Yoshizumi, H., Tatematsu, A., Maeda, K., Ohara, M., Tomiyama, S., and Niimura, K. (1995) Elevated serum levels of 3-deoxyglucosone, a potent protein-cross-linking intermediate of the Maillard reaction, in uremic patients. *Nephron 69*, 438–443.

(6) Beisswenger, P. J., Howell, S. K., Nelson, R. G., Mauer, M., and Szwergold, B. S. (2003) α-Oxoaldehyde metabolism and diabetic complications. *Biochem. Soc. Trans. 31*, 1358–1363.

(7) Nakayama, T., Hayase, F., and Kato, H. (1980) Formation of ε-(2-formyl-5-hydroymethyl-1-yl)-L-norleucine in the Maillard reaction between D-glucose and L-lysine. *Agric. Biol. Chem. 44*, 1201–1202.

(8) Basta, G., Schmidt, A. M., and Caterina, R. D. (2004) Advanced glycation end products and vascular inflammation: Implications for accelerated atherosclerosis in diabetes. *Cardiovasc. Res. 63*, 582–592.

(9) Omura, H., Jahan, N., Shinohara, K., and Murakami, H. (1983) Formation of mutagens by the Maillard reaction. *ACS Symp. Ser. 215*, 537–563.

(10) Yoshihara, K., Kiyonami, R., Shimizu, Y., and Beppu, M. (2001) Determination of urinary pyrraline by solid-phase extraction and high performance liquid chromatography. *Biol. Pharm. Bull. 24*, 863–866.

(11) Odani, H., Shinzato, T., Matsumoto, Y., Takai, I., Naki, S., Miwa, M., Iwayama, N., Amano, I., and Maeda, K. (1996) First evidence for accumulation of protein-bound and protein-free pyrraline in human uremic plasma by mass spectrometry. *Biochem. Biophys. Res. Commun. 224*, 237–241.

(12) Portero-Otin, M., Pamplona, R., Bellmunt, M. J., Bergua, M., Nagaraj, R. H., and Prat, J. (1997) Urinary pyrraline as a biochemical marker of non-oxidative Maillard reactions in vivo. *Life Sci. 60*, 279–287.

(13) Portero-Otin, M., Pamplona, R., Bellmunt, M. J., Bergua, M., and Prat, J. (1997) Glycaemic control and in vivo non-oxidative Maillard reaction: Urinary excretion of pyrraline in diabetes patients. *Eur. J. Clin. Invest. 27*, 767–773.

(14) La Vecchia, C., Negri, E., Decarli, A., and Francechi, S. (1997) Diabetes mellitus and the risk of primary liver cancer. *Int. J. Cancer 73*, 204–207.

(15) La Vecchia, C., Negri, E., Francechi, S., D'Avanzo, B., and Boyle, P. (1994) A case-control study of diabetes mellitus and cancer risk. *Br. J. Cancer 70*, 950–953.

(16) Rousseau, M. C., Parent, M. E., Pollak, M. N., and Siemiatycki, J. (2006) Diabetes mellitus and cancer risk in a population-based case-control study among from Montreal, Canada. *Int. J. Cancer 1182*, 2105–2109.

(17) Inoue, M., Iwasaki, M., Otani, T., Sasazuki, S., Noda, M., and Tsugane, S. (2006) Diabetes mellitus and the risk of cancer. *Arch. Intern. Med. 166*, 1871–1877.

(18) Ward, P. A., Till, G. O., Kunkel, R., and Beauchamp, C. (1983) Evidence for role of hydroxyl radical in complement and neutrophil-dependent tissue injury. *J. Clin. Invest. 72*, 789–801.

(19) Ramos, C. L., Pou, S., Britigan, B. E., Cohen, M. S., and Rosen, G. M. (1992) Spin trapping evidence for myeloperoxidase-dependent hydroxyl radical formation by human neutrophils and monocytes. *J. Biol. Chem. 267*, 8307–8312.

(20) Ushiyama, H., Wakabayashi, K., Hirose, M., Itoh, H., Sugimura, T., and Nagao, M. (1991) Presence of carcinogenic heterocyclic amines in urine of healthy volunteers eating normal diet, but not of inpatients receiving parenteral alimentation. *Carcinogenesis 12*, 1417–1422.

(21) Zhang, X., Campo, M. A., Yao, T., and Larock, R. C. (2005) Synthesis of substituted quinolines by electrophilic cyclization of *N*-(2-alkynyl)anilines. *Org. Lett. 7*, 763–766.

(22) Shioiri, T., Ninomiya, K., and Yamada, S. (1972) Diphenylphosphoryl azide. New convenient reagent for a modified Curtius reaction and for peptide synthesis. *J. Am. Chem. Soc. 94*, 6203–6205.

(23) Ozeki, M., Muroyama, A., Kajimoto, T., Watanabe, T., Wakabayashi, K., and Node, M. (2009) Synthesis of a new mutagenic benzoazepinoquinolinone derivative. *Synlett. 11*, 1781−1784.

(24) Yahagi, T., Nagao, M., Seino, Y., Matsushima, T., and Sugimura, T. (1977) Mutagenicities of *N*-nitrosamines on *Salmonella*. *Mutat. Res. 48*, 121–129.

(25) Maron, D. M., and Ames, B. N. (1983) Revised methods for the *Salmonella* mutagenicity test. *Mutat. Res. 113*, 173–215.

(26) Watanabe, M., Jr., Ishidate, M., and Nohmi, T. (1990) Sensitive method for detection of mutagenic nitroarenes and aromatic amines: New derivatives of *Salmonella typhimurium* tester strains possessing elevated *O*-acetyltransferase levels. *Mutat. Res. 234*, 337–348.

(27) Wakabayashi, K., Nagao, M., Esumi, H., and Sugimura, T. (1992) Food-derived mutagens and carcinogens. *Cancer Res. 52* (7 Suppl), 2092s–2098s.

(28) Sugimura, T., Wakabayashi, K., Hitoshi, N., and Nagao, M. (2004) Heterocyclic amines: Mutagens/carcinogens produced during cooking of meat and fish. *Cancer Sci. 95*, 290–299.

(29) Jagerstad, M., Olsson, K., Grivas, S., Negishi, C., Wakabayashi, K., Tsuda, M., Sato, S., and Sugimura, T. (1984) Formation of 2-amino-3,8-dimethylimidazo-[4,5-*f*]quinoxaline in a model system by heating creatinine, glycine and glucose. *Mutat. Res. 126*, 239–244.

(30) Shioya, M., Wakabayashi, K., Sato, S., Nagao, M., and Sugimura, T. (1987) Formation of a mutagen, 2-amino-1-methyl-6-phenylimidazo[4,5-*b*]-pyridine (PhIP) in cooked beef, by heating a mixture containing creatinine, phenylalanine and glucose. *Mutat. Res. 191*, 133–138.

(31) Turesky, R. J., Goodenough, A. K., Ni, W., McNaughton, L., LeMaster, D. M., Holland, R. D., Wu, R. W., and Felton, J. S. (2007) Identification of 2-amino-1,7-dimethylimidazo[4,5-*g*]quinoxaline: An abundant mutagenic hetrocyclic aromatic amine formed in cooked beef. *Chem. Res. Toxicol. 20*, 520–530.

TX900119J

Particle and Fibre Toxicology

BioMed Central

Research

Open Access

Genotoxicity of nano/microparticles in *in vitro* micronuclei, *in vivo* comet and mutation assay systems

Yukari Totsuka*[1], Takashi Higuchi[1], Toshio Imai[2], Akiyoshi Nishikawa[3], Takehiko Nohmi[4], Tatsuya Kato[5], Shuich Masuda[5], Naohide Kinae[5], Kyoko Hiyoshi[6], Sayaka Ogo[7], Masanobu Kawanishi[7], Takashi Yagi[7], Takamichi Ichinose[8], Nobutaka Fukumori[9], Masatoshi Watanabe[10], Takashi Sugimura[1] and Keiji Wakabayashi[1]

Address: [1]Cancer Prevention Basic Research Project, National Cancer Center Research Institute, 1-1 Tsukiji 5-chome, Chuo-ku, Tokyo 104-0045, Japan, [2]Central Animal Laboratory, National Cancer Center Research Institute, 1-1 Tsukiji 5-chome, Chuo-ku, Tokyo 104-0045, Japan, [3]Division of Pathology, National Institute of Health Sciences, 1-18-1 Kamiyoga, Setagaya-ku, Tokyo 158-8501, Japan, [4]Division of Genetics and Mutagenesis, National Institute of Health Sciences, 1-18-1 Kamiyoga, Setagaya-ku, Tokyo 158-8501, Japan, [5]Department of Food and Nutritional Sciences, Graduate School of Nutritional and Environmental Sciences, University of Shizuoka, 52-1, Yada, Shizuoka, 422-8526, Japan, [6]Fundamental Nursing, School of Nursing, University of Shizuoka, 52-1, Yada, Shizuoka, 422-8526, Japan, [7]Environmental Genetics Laboratory, Frontier Science Innovation Center, Osaka Prefecture University, 1-2 Gakuen-cho Naka-ku, Sakai-city, Osaka, 599-8570, Japan, [8]Department of Health Sciences, Oita University of Nursing and Health Sciences, 2944-9 Megusuno, Oita-city, Oita, Japan, [9]Department of Environmental Health and Toxicology, Tokyo Metropolitan Institute of Public Health, 24-1, Hyakunin-cho 3-Chome, Shinjuku-ku, Tokyo, 169-0073, Japan and [10]Division of Materials Science and Engineering, Yokohama National University, Graduate School of Engineering, 79-5, Tokiwadai, Hodogaya-ku, Yokohama, 240-8501, Japan

Email: Yukari Totsuka* - ytotsuka@gan2.res.ncc.go.jp; Takashi Higuchi - tahiguch@ncc.go.jp; Toshio Imai - toimai@ncc.go.jp; Akiyoshi Nishikawa - nishikaw@nihs.go.jp; Takehiko Nohmi - nohmi@nihs.go.jp; Tatsuya Kato - p7107@mail.u-shizuoka-ken.ac.jp; Shuich Masuda - masudas@u-shizuoka-ken.ac.jp; Naohide Kinae - kinae@u-shizuoka-ken.ac.jp; Kyoko Hiyoshi - hiyoshi@u-shizuoka-ken.ac.jp; Sayaka Ogo - es04509@riast.osakafu-u.ac.jp; Masanobu Kawanishi - kawanisi@riast.osakafu-u.ac.jp; Takashi Yagi - yagi-t@riast.osakafu-u.ac.jp; Takamichi Ichinose - ichinose@oita-nhs.ac.jp; Nobutaka Fukumori - Nobutaka_Fukumori@member.metro.tokyo.jp; Masatoshi Watanabe - mawata@ynu.ac.jp; Takashi Sugimura - tsugimur@ncc.go.jp; Keiji Wakabayashi - kwakabay@ncc.go.jp

* Corresponding author

Published: 3 September 2009

Particle and Fibre Toxicology 2009, **6**:23 doi:10.1186/1743-8977-6-23

Received: 1 May 2009
Accepted: 3 September 2009

This article is available from: http://www.particleandfibretoxicology.com/content/6/1/23

Abstract

Background: Recently, manufactured nano/microparticles such as fullerenes (C_{60}), carbon black (CB) and ceramic fiber are being widely used because of their desirable properties in industrial, medical and cosmetic fields. However, there are few data on these particles in mammalian mutagenesis and carcinogenesis. To examine genotoxic effects by C_{60}, CB and kaolin, an *in vitro* micronuclei (MN) test was conducted with human lung cancer cell line, A549 cells. In addition, DNA damage and mutations were analyzed by *in vivo* assay systems using male C57BL/6J or *gpt* delta transgenic mice which were intratracheally instilled with single or multiple doses of 0.2 mg per animal of particles.

Results: In *in vitro* genotoxic analysis, increased MN frequencies were observed in A549 cells treated with C_{60}, CB and kaolin in a dose-dependent manner. These three nano/microparticles also induced DNA damage in the lungs of C57BL/6J mice measured by comet assay. Moreover, single or multiple instillations of C_{60} and kaolin, increased either or both of *gpt* and Spi$^-$ mutant frequencies in the lungs of *gpt* delta transgenic mice. Mutation spectra analysis showed transversions were

predominant, and more than 60% of the base substitutions occurred at G:C base pairs in the *gpt* genes. The G:C to C:G transversion was commonly increased by these particle instillations.

Conclusion: Manufactured nano/microparticles, CB, C_{60} and kaolin, were shown to be genotoxic in *in vitro* and *in vivo* assay systems.

Background

Nano/microparticles are widely used because of their desirable properties in industrial, medical and cosmetic fields [1-6]. Accordingly, these particles can be released into the human environment and then can be inhaled. Most exposure to airborne nano/micromaterials occurs in the work place. Nano/microparticles can be classified into three groups: natural, anthropogenic and man-made (or artificial). The natural kind, for example, is produced during forest fires or volcanic eruptions. Anthropogenic particles are quite often a by-product of industrial activities such as welding or polishing. Diesel exhaust products, PM10 and PM2.5, well known as combustion nanoparticles, also belong to this group. The man-made group includes engineered nanomaterials [5].

Among these nano/mocroparticles, diesel exhaust particles have been well documented, in their general toxicity, mutagenicity and carcinogenicity [7-10]. In addition, asbestos, a naturally occurring nano-sized silicate mineral fiber, has been considered to be a human carcinogen [11-13]. Animal experiments and epidemiological studies have already demonstrated that pulmonary fibrosis, bronchogenic carcinomas and malignant mesotheliomas are closely associated with asbestos exposure. Another mineral fiber, titanium dioxide (TiO_2) has also been subjected to extensive research, and TiO_2 has already been shown to be carcinogenic [14]. Moreover, man-made vitreous fibres, including glass fibres, refractory ceramic fibres, and rock wool, have been sorted as carcinogens [15]. Kaolin/kaolinite is a clay mineral with the chemical composition $Al_2Si_2O_5(OH)_4$, and is used in ceramics, medicines, food additives, toothpaste and cosmetics. The largest use of kaolin is in the production of paper [3]. In 1993, W. B. Bunn 3rd *et al.* reported that increased incidences of lung tumors and mesotheliomas were observed in long-term inhalation studies of rats and hamsters treated with micro-sized refractory ceramic fibres containing kaolin as the main component [16]. However, other genotoxic and carcinogenic potentials of kaolin have not been studied *in vitro* and *in vivo*. In addition, the mechanism of cancer development by kaolin is still unclear.

On the other hand, carbon black (CB), fullerenes (C_{60}) and carbon nanotubes (CNTs) are developed as engineered nanoproducts [1,2,6,17]. Despite their highly desirable structures, their toxicity and carcinogenicity are concerns because these engineered nanoproducts are considered to be very stable and could lead to continuous inflammation when deposited in tissues. CNTs especially have received much attention from the aspect of toxicity due to their asbestos-like rod-shaped particles, and iron content [17-19]. Recently Takagi *et al.* demonstrated that multi-wall carbon nanotubes induced mesothelioma in *p53*+/- mice by a single i.p. injection [20]. In contrast, C_{60} is a spherical molecule consisting entirely of carbon atoms, and various derivatives have been reported [6,21,22]. C_{60} has widely different properties, such as scavenging of reactive oxygen species, direct interaction with biomolecules and radical formation; however, clear genotoxic and carcinogenic effects have not yet been demonstrated.

The present study aims to examine the genotoxicity/clastogenicity of widely distributed nano/microparticles such as C_{60}, CB and kaolin by an *in vitro* micronucleus test. Moreover, we analyzed the genotoxic effects of these particles by an *in vivo* comet assay and mutation assay system using *gpt* delta transgenic mice. In this mouse model, point mutations and deletions are separately analyzable by *gpt* and Spi- selections, respectively [23,24]. The mutation assay using the *gpt* delta mouse was validated and so far is widely used in the field of environmental mutagenicity.

Results

Size distribution and agglomeration state in suspensions of nano/microparticles

Figure 1 shows representative transmission electron microscope (TEM) images for the state of test materials

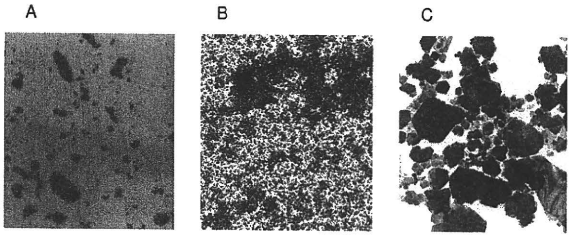

Figure 1
Representative TEM images of the presently used nano/microparticles within the suspensions. C_{60} (PanelA), CB (Panel B) and kaolin (Panel C) were suspended in saline containing 0.05% Tween 80 at a concentration of 2 mg/mL with a 10 min sonication. All images are shown at the original magnification of × 10,000.

dispersed in saline containing 0.05% Tween 80. These were commonly observed to be a mixture of well dispersed fine particles and agglomerates. C_{60} was frequently agglomerated, but fine particles were also observed either individually or within pear-shaped agglomerates. In contrast, CB was relatively well dispersed, and agglomerates were occasionally present. In the case of kaolin, low-density tabular structures with rectangular or hexagonal shape were characteristically observed. The size distribution of materials used in the present study was analyzed by dynamic light scattering (DLS). C_{60} demonstrated a wide distribution with ranges of 10.5 to 12913.9 nm, and most abundant sizes were two peaks at 234.1 ± 48.9 and 856.5 ± 119.2 nm, respectively. CB particles formed a normal distribution with ranges of 13.6 to 337.4 nm and major peak average was at around 232.0 nm. In the case of kaolin, a major peak average was 357.6 ± 199.4 nm belonging to a range of 5.1 to 4846.9 nm. Although the primary particle size of kaolin was 4.8 μm, it is likely that sonication might lead to size reduction.

In vitro *micronucleus test*

To examine the genotoxicity of particles, we analyzed the micronucleus inducing activity of C_{60}, CB and kaolin using human lung cancer cell line, A549. A six-hour treatment of 200 μg/mL CB and kaolin caused growth inhibition of 60% in A549 cells; however, C_{60} did not inhibit growth of cells at any concentrations (between 0.02 - 200 μg/mL, data not shown). As shown in Figure 2, C_{60} and kaolin particles increased the number of micronucleated cells in a dose-dependent manner. On the other hand, CB increased the number of micronucleated cells up to 2 μg/mL, and thereafter seemed to plateau. The background frequency of micronucleated cells was 0.7% to 1.0%, and the frequency rose to 10% and 5% at 200 μg/mL of C_{60} and kaolin, respectively, and 3.3% at 2 μg/mL of CB treatment. The increase of the frequency from that of the control cells was statistically significant in all particle-treated cells. C_{60} demonstrated the most strong genotoxic/clastogenic potencies among these three particles.

In vivo *genotoxicity analyzed by alkaline comet assay*

DNA damage induced by particles was evaluated using comet assay under alkaline conditions. Figure 3 shows the mean values of DNA tail moment in the lungs with or without single-particle treatment at 0.2 mg/body for 3 hr. In the case of particle exposure, DNA damage was significantly increased as compared with the vehicle control up to 2 - 3 fold, and its intensity was C_{60} > CB > kaolin. On the other hand, we examined the genotoxicity of nano/microparticles at a dose of 0.05 mg/animal. DNA damage observed in the lung of mice was almost the same as those of the vehicle control (data not shown). Moreover, we examined the effects of different exposure times for 3 and 24 hr. While DNA damages induced by CB or kaolin were not changed either for 3 or 24 hr, DNA damage caused by C_{60} was decreased for 24 hr compared with 3 hr (data not shown). It seems that DNA damage repair enzymes might affect the result of comet assay.

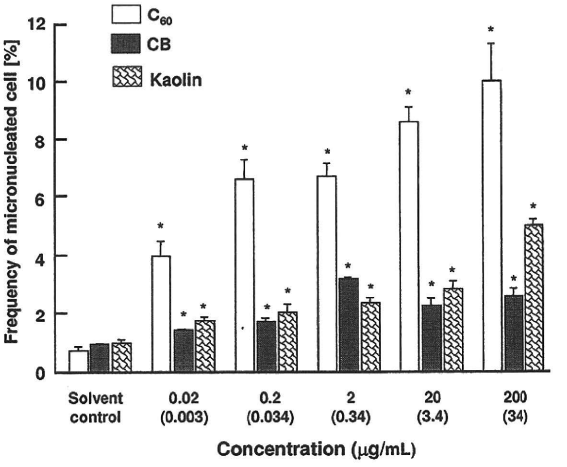

Figure 2
Frequency of micronucleated A549 cells incubated with C_{60} CB or kaolin. The values represent the mean of three experiments ± SD. An asterisk (*) represents that each frequency is significantly different ($p < 0.01$) from that of control cell in a Student's t-test. Concentrations in μg/cm² are given in parenthesis.

General observations of gpt *delta transgenic mice administrated with particles*

Body weights of *gpt* delta mice receiving a single dose of vehicle control reached 31.1 ± 1.8 g at 12 weeks after instillation. Values for *gpt* delta mice which received a single dose of particles at 0.2 mg/body were 30.0 ± 2.4 g for C_{60}, 32.6 ± 1.1 g for CB and 30.8 ± 2.3 g for kaolin, respectively, at 12 weeks after instillation. The average consumption of diet per day per mouse was 3.6 g, with no effects from particle instillation. No body weight and diet consumption changes were also observed with multiple doses of particles. All mice used for the single dose study survived to the end of the study, although, in the case of multiple doses, one fullerene- and one kaolin-administrated mouse died within two weeks after the last instillation, probably due to respiratory disturbances.

gpt *Mutations in the lungs of* gpt *transgenic mice with particle treatment*

To determine the mutagenic effects of particles in the lungs, *gpt* delta transgenic mice were exposed to C_{60}, CB and kaolin at doses of 0.2 mg/body by single intratracheal instillation, and mutations were analyzed. Figure 3 shows the mutant frequencies (MFs) of the lungs. The back-

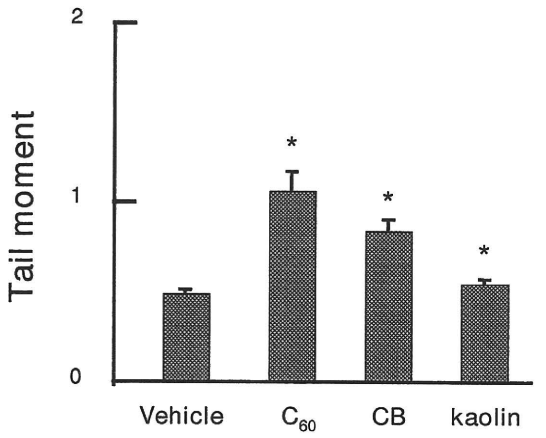

Figure 3
DNA damage in lungs of C57BL/6J mice intratracheally instilled with particles. DNA damage was measured by comet assay. Male mice were treated at a dose of 0.2 mg per animal of particles, and mice were sacrificed 3 hr after particle administrations. The values represent the mean of five animals ± SE. An asterisk (*) denotes $p < 0.01$ in a Dunnett's test after one-way ANOVA of Tail Moment of particle-treated vs. corresponding vehicle-control mice.

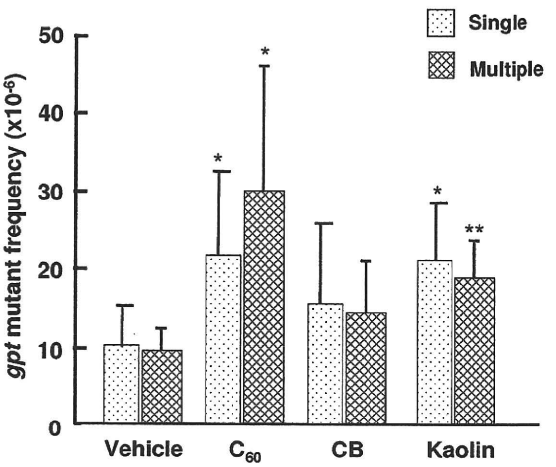

Figure 4
***gpt* MFs in the lungs of mice singly and multiply intratracheally instilled with particles.** Male mice were treated with single (0.2 mg per animal) or multiple (0.2 mg per animal × 4) doses of particles, and mice were sacrificed 12 (single) and 8 (multiple) weeks after particle administrations. Mean values ± SD are shown. An asterisk (*, **) denotes $p < 0.05$ (*) and $p < 0.01$ (**) in a Student's *t*-test of MF of particle-treated vs. the corresponding vehicle-control mice.

ground MF of lungs was 10.30 ± 0.53 × 10^{-6}. MFs in the lungs induced by C_{60} and kaolin were significantly increased by 2-fold compared with vehicle-instilled animals. CB showed increasing tendency for MF in the lungs, but not statistically significant.

Next, we examined the mutagenic effects of consecutive exposure of particles. The *gpt* MFs in the lungs obtained from mice multiply exposed (4 times) to 0.2 mg/body each of C_{60}, CB or kaolin are shown in Figure 4. In cases of C_{60} and kaolin, MFs of the lungs were significantly higher as compared to those of control animals, and their values were 2 - 3 fold increased. In the case of CB exposure, MFs were slightly increased but not statistically significant.

To analyze the mutational characteristics induced by particles, we examined PCR and DNA sequencing analysis of 6-thioguanine (6-TG)-resistant mutants. More than 40 independent 6-TG resistant mutants derived from multiple particle instillation (0.2 mg × 4), and 25 mutants from vehicle instilled animals were identified. Classes of mutations found in the *gpt* gene are listed in Table 1. Base substitutions predominated with both particle-induced and spontaneous cases. No A:T to T:A and G:C to C:G transversions were detected in vehicle control groups, indicating that these types of mutations are rare events in the spontaneous mutations. Interestingly, G:C to C:G transversion commonly increased in all three particle treatments compared to the vehicle control. G:C to A:T transition also significantly increased in CB and kaolin instillation but not in C_{60}. In addition, the numbers of A:T to T:A transversion were slightly increased in the treatment with C_{60} and CB. Other types of mutations, including deletions and insertions, were also observed in both particle-treated and vehicle control groups, but these were of minor significance.

The distribution of spontaneous and particle-induced mutations in the *gpt* gene is shown in Figure 5. Base substitutions were spread throughout the coding region with a preference for some sites. However, clear mutational hotspots for each particle could not be seen except deletion mutations occurring at a run of 5 adenines (positions 8 to 12) and at position 244 for C_{60} treatment. The distribution of base substitutions along the *gpt* gene did not vary with the particle types. Twelve out of 200 particle-induced mutations occurred at position 64, eighteen at position 110, ten at position 115. All of the base substitutions occurring at positions 110 and 115 were G to A transitions, and at position 64 were C to T transitions, which were common among spontaneous mutants. In contrast, four to eight mutations occurred at positions 116, 143,

Table 1: Classification of *gpt* mutations from the lungs of control and particle multiply (0.2 mg × 4) treated mice[a)]

	Control		C_{60}		CB		Kaolin	
Type of mutation in gpt	No.	%	No.	%	No.	%	No.	%
Base substitutions								
Transitions	10	40	35	41	18	45	37	50
A:T->G:C	2	8	11	13	2	5	5	7
G:C->A:T	8	32	24	28	16	40	32	43
Transversions	10	40	35	40	17	43	30	41
A:T->T:A	0	0	2	2	1	3	0	0
A:T->C:G	2	8	3	3	4	10	5	7
G:C->T:A	8	32	25	29	8	20	17	23
G:C->C:G	0	0	5	6	4	10	8	11
Deletions	4	16	12	14	4	10	6	8
Insertions	1	4	3	4	0	0	1	1
Others	0	0	1[b)]	1	1[c)]	3	0	0
Total	25	100	86	100	40	101	74	100

[a)]Independent mutations were isolated no more than once from any individual mouse.
[b)]Multiple mutation (Four base substitutions)
[c)]Tandem mutation (GG->TT)

189, 320, 406 and 418 were only seen in the particle-treated mice, therefore it is suggested that these mutations can be considered as particle-induced mutations. Among these, five out of six mutations at position 406 were found in C_{60} instillation, and all mutation patterns were G to T transversions. Four out of 7 and five out of 8 at positions 189 and 418 were detected in kaolin instillation, and the majorities of the mutations were G to A and C to A, respectively. Moreover, these hotspots induced by particles occurred at G or C residues in the *gpt* gene without association for specific sequences.

Spi⁻ MFs in the lungs of gpt *transgenic mice with particle treatment*

We also measured the Spi⁻ MFs in the lungs of *gpt* delta mice instilled with multiple doses (0.2 mg × 4) of particles (Figure 6). Spi⁻ MFs of the vehicle control was 4.85 ± 2.04 × 10^{-6}, in contrast, particle-administrated groups were 4.91 ± 3.03 × 10^{-6} for C_{60}, 6.87 ± 4.06 × 10^{-6} for CB and 8.12 ± 3.32 × 10^{-6} for kaolin. As shown in Figure 6, Spi⁻ MFs in the lungs of the CB- and kaolin-treated, but not C_{60}-treated groups were increased, and in particular, the values of the kaolin-treated groups were significantly elevated up to 2-fold.

gpt *Mutations in the kidneys of* gpt *transgenic mice with particle treatment*

To determine the tissue distribution and specificity of particles with intratracheal instillation, *gpt* MFs of the kidney were analyzed. *gpt* MFs of the vehicle control versus particle-multiple administrated groups (0.2 mg × 4) were 1.33 ± 0.51 × 10^{-5} versus 1.67 ± 0.66 × 10^{-5} for C_{60}, 1.03 ± 0.39 × 10^{-5} for CB and 1.32 ± 0.32 × 10^{-5} for kaolin. From these observations, it is suggested that these particles did not induce mutation in the kidneys under these conditions.

Histopathological evaluation

Histopathological analyses of lung tissues of *gpt* delta mice consecutively instilled particles, C_{60}, CB and kaolin, at 0.2 mg/body per week for 4 weeks each are shown in Figure 7. Test substances-phagocytized alveolar macrophages were diffusely found in the lungs, but not in the vehicle group. Focal granulomatous formation accompanied with or without the test substance-phagocytized macrophages were also frequently observed in the lungs of particle-multiply-instilled mice. Similar findings, but a slight degree of particle accumulation and granuloma formation, were also observed in lungs of mice with particle single-instillations (data not shown). The degree of granuloma formation in the lungs of multiple C_{60}- or CB-exposed mice appeared more severe than those in multiple kaolin-exposed mice. No abnormalities were observed in the kidneys obtained from mice multiply instilled with particles (data not shown).

Discussion and conclusion

This study demonstrated the genotoxicity of nano/microparticles widely used for industrial, cosmetic and medical fields. In *in vitro* genotoxic analysis, increased MN frequencies were observed in A549 cells treated with C_{60}, CB and kaolin in a dose-dependent manner. On the other hand, these three particles also induced DNA damage in the lungs of C57BL/6J mice measured by comet assay. Furthermore, we found that C_{60} and kaolin demonstrated mutagenicity either or both of *gpt* and Spi⁻ mutations in the *gpt* delta transgenic mice systems. The *gpt* gene MFs were significantly increased in the lungs of *gpt* delta mice with C_{60} and kaolin, but not CB administrations. A dose-dependent MF increase was observed in the lungs of C_{60}, but not kaolin treated groups. The reason is still unclear, but suggesting that the single dose of kaolin already repre-

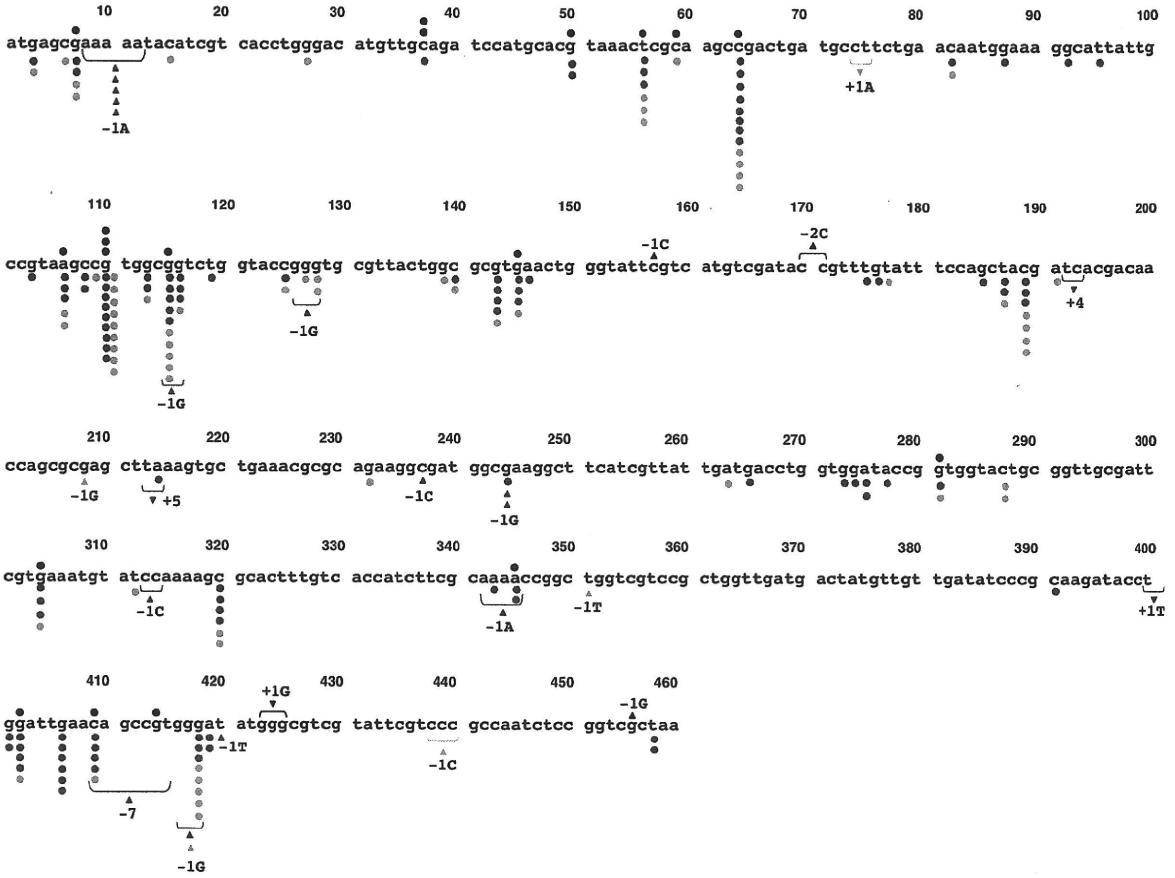

Figure 5

Spontaneous and particle-induced mutations in the coding region of the *gpt* gene. Mutations obtained from the control mice are shown above the wild type sequence, and mutations obtained from the particle-treated mutant clone are shown below the wild type sequence. The types of particles are indicated by color coding: red for C_{60}, blue for CB and sky blue for kaolin. Mutation types, base substitution, and deletion and insertion are indicated by circle, triangle, and inverted triangle, respectively.

sented the maximum response. On the other hand, kaolin demonstrated significantly increased Spi- MFs; however, C_{60} showed similar values compared with the vehicle control of the lungs. Spi- selection detects deletions in size more than 1 bp and 10 kb [24]; therefore, additional DNA damages involved in deletion mutations might be induced by kaolin. It, it is also suggested that C_{60} does not prefer to induce such kinds of DNA damages under these conditions. In contrast to the present study, Xu *et al.* have reported that C_{60} dramatically increases large deletion mutations in *gpt* delta transgenic mouse primary embryo fibroblast cells [25]. The observed difference of mutational signatures of C_{60} between a cell line and lung tissue might be related to differences between *in vitro* and *in vivo* assay systems in DNA damage formations, DNA repair or translesion DNA synthesis.

To further elucidate the mechanisms behind the increase in mutant frequency observed in this study, we analyzed mutation spectra using a PCR-direct sequencing method. Most mutations induced by three particles in the present study, occurred at G:C base pairs (52/76, 68%). Among these, 13 G:C base pairs were located in the G or C runs. The most prominent hot spots were at base pairs 143, 189, 320, 406 and 418, and there were no significant differences in the distributions of mutation hot spots in the three particles. This may reflect the distribution of DNA damage sites caused by particles. The most prominent mutation type induced by particles was G:C to C:G transversion. Since these mutations were commonly increased regardless of the constituents of particles (i.e. C_{60} and CB were graphite and kaolin was aluminum silicate), it is suggested that mechanisms leading to the induction of such

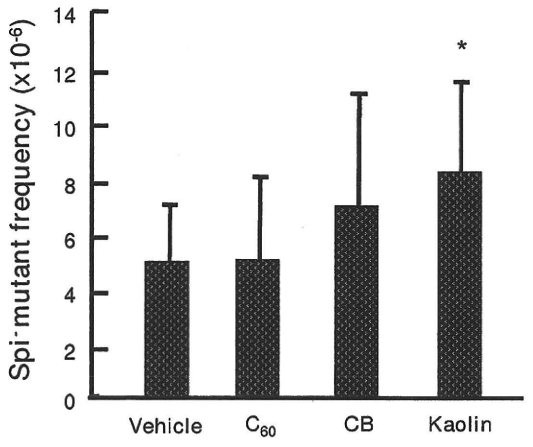

Figure 6
MFs of deletions in the lungs of *gpt* delta mice exposed to multiple doses of particles. An asterisk (*) denotes $p < 0.05$ in a Student's *t*-test of MFs of particle-treated vs. the corresponding vehicle-control mice.

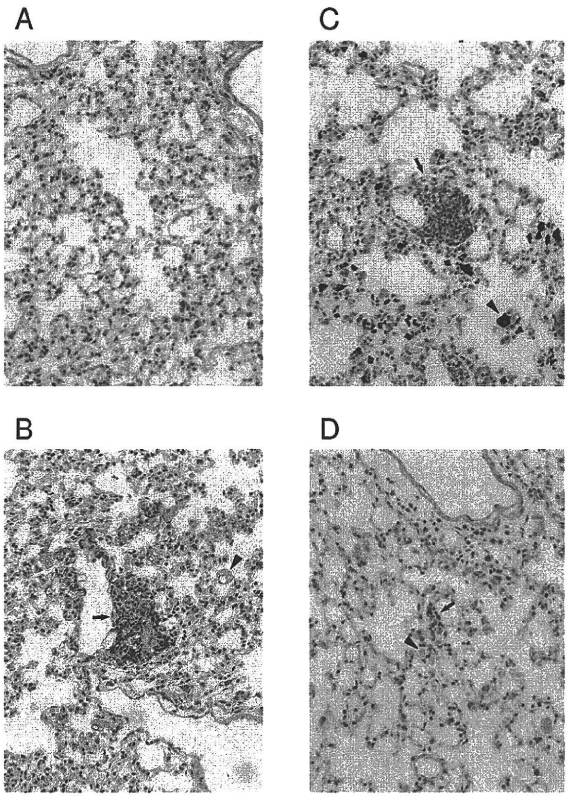

Figure 7
Microscopic findings in lungs of *gpt* delta mice intratracheally instilled with particles. Normal appearance of pulmonary parenchyma in a vehicle-control (Panel A). Pulmonary parenchyma obtained from *gpt* delta mice intratracheally instilled with four consecutive doses of 0.2 mg/mice of C_{60} (Panel B), CB (Panel C) and kaolin (Panel D). Test substance-phagocytized macrophages (arrowheads) can be observed, and granulomaous (arrows) formations are also found in lungs of particle-instilled mice. A-D; Original magnification × 40.

kinds of mutations might be same. In general, the G:C to C:G transversion is thought to be a rare event in both spontaneous and chemically-induced mutations. However, various oxidative stresses caused by sunlight, UV radiation, hydrogen peroxide and peroxy radicals frequently induce G:C to C:G transversion in *in vitro* assay systems [26-29]. Reactive oxygen species (ROS) and DNA damage, including 8-oxo-7,8-dihydro-2'-deoxyguanosine (8-oxo-dG), were reported to be increased by nanoparticles, including asbestos, treatment [4,21,30-34]. The mechanism of the generation of ROS by nanoparticles is still unclear; however, these nanoparticles would be able to trigger ROS production by iron-catalysed Fenton reactions, or would be accumulated in the cells by phagocytosis, then enhance the production of ROS from macrophages and leucocytes [35,36]. In the present study, test substance-phagocytized macrophages and granulomas were frequently observed in the lungs, and the degree of the granulomas formation was partly associated with the mutagenic effect on *gpt* gene by particles. In the case of C_{60}, generation of ROS along with lipid peroxidation via electron transfer between C_{60} and other molecules has been reported [21]. The most typical lesion of oxidative damage is 8-oxo-dG which can pair with dA and leads G to T transversions [37,38] but it is not responsible for G to C transversion since dG is not incorporated opposite 8-oxodG [37,39]. Moreover, a variety of oxidative lesion products of guanine other than 8-oxodG, including imidazolone (Iz), oxazolone (Oz), spiroiminodihydantoin (Sp) and guanidinohydantoin (Gh), have been reported [39-45]. Recently, three such molecules, Oz, Sp and Gh are thought to be the key molecules causing G to C transversion using the translesion synthesis systems [43-46]. Moreover, these molecules have also been detected in bacterial cells and rat liver [47,48]. Therefore, it is suggested that G:C to C:G transversions induced by particles such as C_{60}, CB and kaolin could involve Oz, Sp and Gh formations.

In the present study, G:C to A:T transition and A:T to T:A transversion were also increased in the particle treatment. G to A transition has commonly been observed in spontaneous and chemically-induced mutants and deamination of 5-methylcytosine or alkylation of guanine might be

involved in these mutations. In contrast to G to A transition, A:T to T:A transversion is known as a rare mutation. It has been reported that the most common mutations induced by N-ethyl-N-nitrosourea in the mouse are A:T to T:A transversions [49]. However, at present, the mechanisms underlying generation of A to T transversion by particles are still unclear.

As mentioned above, we found that all three particles, C_{60}, CB and kaolin increased significant DNA damage in the lungs compared to the vehicle control using the comet assay. Comet assay under alkaline conditions is used to detect both strand breaks and DNA altering lesions such as an AP site [50]. Moreover, in the present study, treatments with C_{60}, CB and kaolin significantly increased the frequency of micronucleated A549 cells in a dose-dependent manner. However, these genotoxic/clastogenic potencies did not necessarily correspond to the mutagenicity observed in *gpt* transgenic mice.

In conclusion, we demonstrated that manufactured nano/microparticles such as C_{60}, CB and kaolin were shown to be genotoxic in both *in vitro* and *in vivo* assay systems. Moreover, it was not necessarily the case that genotoxic potency was related to particle size (C_{60} and CB are nano-sized, but kaolin is micro-sized particles used in the present study.). From the prominent mutation spectra, it is suggested that oxidative DNA damage might be commonly involved in their mutagenicity. The dose of particles used in the present study seems to be extremely high compared with human exposure in the work place. However, it is likely that these materials would be deposited for a long time in tissues, same as those of asbestos fiber. Therefore, further studies of the mechanisms of genotoxicity and application routes other than trachea are needed. Moreover, exposure levels of these genotoxic particles in the working environment should be determined.

Materials and methods

Materials and chemicals

CB nanoparticles with a primary particle size of 14 nm (Printex 90) were obtained from Degussa, Dusseldorf, Germany. The surface area was 300 m^2/g (disclosed by Degussa). The CB was autoclaved at 250°C for 2 h before use. High purity (99.9%) C_{60} was purchased from Sigma-Aldrich. (St. Louis, MO, USA). The declared primary particle size of C_{60} was 0.7 nm. Kaolin, white crystal, with a primary particle size of 4.8 μm was obtained from Engelhard Corp., Iselin, NJ. C_{60}, CB and kaolin particles were suspended in saline (Otsuka Pharmaceutical Co. Ltd., Tokyo, Japan) containing 0.05% of Tween 80 (Nacalai Tesque, Kyoto, Japan) by sonication for 15 - 20 min, at a concentration of 2 mg/mL. The size distributions of the presently used nano/microparticles in the suspensions were measured by dynamic light scattering (DLS) using FPAR-1000 (Otsuka electronics Co., Ltd., Osaka), and the agglomeration state was assessed by transmission electron microscope (TEM) (H-7000, Hitach, Ltd., Tokyo, Japan). The size distributions were determined with the algorithm CONTIN. For the TEM assessment, an aliquot of 5 μL was put on the nickel glid coated by hydrophilized formbar and assessed with an accelerating voltage of 75 kV.

Type I agarose, low melting point agarose, dimethylsulfoxide and Triton X-100 were bought from Sigma-Aldrich. Ethidium bromide was obtained from Merck (Darmstadt, Germany). Other chemicals were purchased from Wako Pure Chemical Industries (Osaka, Japan).

Micronucleus test

Human lung carcinoma A549 cells obtained from the RIKEN Cell Bank (Wako, Japan) were cultured in Eagle's minimum essential medium (Nissui Pharmaceutical Co. Ltd., Tokyo, Japan) supplemented with 10% fetal bovine serum (JRH Biosciences, Lenexa, KS, USA) in a 5% CO_2 atmosphere at 37°C. The cells (7×10^5 cells/dish) were seeded in plastic cell culture dishes (ϕ60 mm) one day before treatment. Particles were suspended in physiological saline containing 0.05% (v/v) Tween-80 with sonication (for 5-10 min at room temperature). One volume of the suspension was mixed with 9 volumes of the culture medium with serum (altogether 3.3 mL/dish), and then cells were treated at indicated concentrations for 6 hr. Since a long exposure (48 hr) increased the frequency of micronucleated cells in the solvent control (data not shown), we chose a 6 hr treatment. After treatment, cells were further cultured for 42 hr. Then, cells were trypsinized and counted, and centrifuged. Growth inhibition was calculated by following the formula:

Growth rate = (the number of treated cells) /(the number of non-treated cells)

Cells were resuspended in 0.075 M KCl, and incubated for 5 min. Cells were then fixed 4 times in methanol:glacial acetic acid (3:1), and washed with methanol containing 1% acetic acid. Finally, cells were resuspended in methanol containing 1% acetic acid. The cell solution was dropped onto slides and the nucleus was stained by mounting with 40 μg/mL acridine orange (Nacalai Tesque) solution and immediately observed by fluorescence microscopy using blue excitation. The number of cells with micronuclei was recorded based on observation of 1,000 interphase cells. The data of EMS and mitomycine C (MMC) for positive system controls in CHL cells under the same experimental conditions were as follows; Percentage of micronucleated cells were 9.8 ± 0.68 for EMS (1 mg/mL) and 10.3 ± 1.1 for MMC (100 n/mL), respectively.

Animals

Male C57BL/6J mice (9 weeks old) were purchased from Charles River Japan, Inc. (Atsugi, Japan) and *gpt* delta mice (9 weeks old) were obtained from Japan SLC (Shi-

zuoka, Japan), respectively. The *gpt* delta mice carry approximately 80 copies of *lambda* EG10 DNA on each chromosome 17 on a C57BL/6J background [23]. Animals were provided with food (CE-2 pellet diet, CLEA Japan, Inc., Tokyo, Japan) and tap water *ad libitum* and quarantined for one week. Mice were maintained under controlled conditions: 12-h light/dark cycle, 22 ± 2°C room temperature, and 55 ± 10% relative humidity. The experiments were conducted according to the "Guidelines for Animal Experiments in the National Cancer Center" of the Committee for Ethics of Animal Experimentation of the National Cancer Center.

Treatment of wild type and gpt *delta transgenic mice with particles*

All particles were well sonicated and suspended in saline containing 0.05% of Tween 80. For comet assay, 5 male C57BL/6J mice were intratracheally instilled with particles using a polyethylene tube under anesthesia with 4% halothane (Takeda Chemical, Osaka, Japan). Single doses of 0.05 or 0.2 mg per animal were employed. The control mice (n = 5) were instilled intratracheally with 0.1 mL of the solvent alone. The mice were sacrificed 3 hr after these particle administrations, and lungs were removed then used for comet assay immediately. In addition, different exposure time (24 hr) was also examined. For histological and mutation analysis, each group of 10 male *gpt* delta mice was intratracheally instilled with particles at a single dose of 0.2 mg per animal, and multiple doses of 0.2 mg per animal per week for 4 consecutive instillations, as described for comet assay. The intratracheal instillation dose of particles between 0.05 and 1 mg/mouse has been commonly used for the pulmonary inflammation and genotoxicity test [51,52]. The control mice (n = 10) were instilled intratracheally with the solvent alone. The mice were sacrificed at 22 weeks old being 12 (for single instillation) or 8 (for multiple instillations) weeks after particle administrations, respectively. Tissues, including lungs and kidneys, were removed. Lungs and kidneys obtained from 4 mice were used for histological evaluation and examined under a light microscope for any abnormalities. For histopathological evaluation, organs were fixed in 10% neutral buffered formalin, embedded in paraffin blocks and routinely processed to H&E stained sections. The remaining 6 mice were used for mutation analysis and the tissues were stored at -80°C until the DNA was isolated.

Alkaline comet assay

The alkaline comet assay was performed according to the method of Sasaki et al. [53] or Toyoizumi et al. [54] with some modification. The lungs were taken from treated mice and weighed, and lung tissue was minced and suspended with chilled homogenizing buffer, then homogenized gently using a Dounce-type homogenizer in ice. Lung cell suspension was mixed with the same volume of 1.4% low melting point agarose in PBS. The mixture was layered on the slide coated with 0.7% agarose layer, and then covered with 0.7% low melting point agarose. After slide preparation, slides were immersed in lysing solution and refrigerated at 4°C for 1 h. Each slide was then placed in alkaline electrophoresis buffer for 10 min to allow for DNA unwinding. Electrophoresis was performed at 25 V, 300 mA for 15 min at 0°C. The slides were neutralized with Tris buffer for 5 min twice, and dehydrated with 70% ethanol to fix. The cells were stained with ethidium bromide solution. Comet images were analyzed using a fluorescence microscope (magnification 200×) equipped with a CCD camera. Fifty cells were examined per mouse. The tail moment of DNA was measured using Comet Analyzer Youworks Bio Imaging Software.

gpt and Spi⁻ mutation assays

High-molecular-weight genomic DNA was extracted from the lungs and kidneys using a RecoverEase DNA Isolation Kit (Stratagene, La Jolla, CA) according to the instruction manual provided by the supplier. *Lambda* EG10 phages were rescued using Transpack Packaging Extract (Stratagene).

The *gpt* mutagenesis assay was performed according to previously described methods [55]. Briefly, *E. coli* YG6020 was infected with the phage and spread on M9 salt plates containing Cm and 6-TG, then incubated for 72 hr at 37°C. This enabled selection of colonies harboring a plasmid carrying the gene for chloramphenicol acetyltransferase, as well as a mutated *gpt*. Isolate exhibiting the 6-TG-resistant phenotype was cultured overnight at 37°C in LB broth containing 25 mg/mL Cm, then harvested by centrifugation (7,000 rpm, 10 min), and stored at -80°C.

The mutation spectrum of 6-TG cording sequence were performed by PCR and direct sequencing. Briefly, a 739 bp DNA fragment containing *gpt* was amplified by PCR as described previously [30,53]. Sequencing analysis was done at Takara Bio Inc. (Mie, Japan).

The Spi⁻ assay was performed as described previously [53]. The lysates of Spi⁻ mutants were obtained by infection of *E. coli* LE392 with the recovered Spi⁻ mutants. *gpt* and Spi⁻ MFs were determined in each mouse and the means ± standard deviations were calculated.

Statistical analysis

The data from micronucleus test and *gpt* and Spi⁻ mutation assay are expressed as mean ± standard deviations. The data obtained from comet assay are expressed as mean ± standard errors. The data were statistically compared with the corresponding solvent control using the Student's t-

test for micronucleus and *gpt* and Spi- mutation assay. To test for significant differences of tail moment in the comet assay between a group treated with materials and an untreated group, Dunnett's test after one-way ANOVA was used to evaluate the differences; p values lower than 0.05 were considered to indicate statistical significance.

Abbreviations

CB: carbon black; C_{60}: fullerenes; MN: micronuclei; CNTs: carbon nanotubes; TEM: transmission electron microscope; DLS: dynamic light scattering; MFs: mutant frequencies; 6-TG: 6-thioguanine; 8-oxo-dG: 8-oxo-7,8-dihydro-2'-deoxyguanosin; Iz: imidazolone; Oz: oxazolone; Sp: spiroiminodihydantoin; Gh: guanidinohydantoin; ROS: reactive oxygen species.

Competing interests

The authors declare that they have no competing interests.

Authors' contributions

YT carried out the preparation and performance of *gpt* delta transgenic mouse experiments and drafted the manuscript. SO and MK performed *in vitro* MN tests. TK and SM performed the comet assay. TI, KH and TH performed the animal exposure and *gpt* and Spi- mutation analysis. Pulmonary and renal histopathological evaluations were done by TI and AN. Analysis of size distribution and agglomeration state of particles were done by MW and NF. TN, NK, TY, TS and KW conceived and supervised the study. All authors read and approved the final manuscript.

Acknowledgements

We thank Mr. Naoaki Uchiya, Ms Hiroko Suzuki, Yoko Matsumoto, Naoki Itcho and Mitsuyo Fujii for excellent technical assistance. This study was supported by Grants-in-Aid for Cancer Research and for Research on Risk of Chemical Substances from the Ministry of Health, Labour, and Welfare of Japan. Takashi Higuchi one of authors, is an awardee of a Research Fellowship from the Japan Food Hygiene Association for Promoted Project of Research on Risk of Chemical Substances from the Ministry of Health, Labour, and Welfare of Japan.

References

1. Mazzola L: **Commercializing nanotechnology.** *Nat Biotechnol* 2003, **21**:1137-1143.
2. Paull R, Wolfe J, Hebert P, Sinkula M: **Investing in nanotechnology.** *Nat Biotechnol* 2003, **21**:1144-1147.
3. Elmore AR, Cosmetic Ingredient Review Expert Panel: **Final report on the safety assessment of aluminum silicate, calcium silicate, magnesium aluminum silicate, magnesium silicate, magnesium trisilicate, sodium magnesium silicate, zirconium silicate, attapulgite, bentonite, Fuller's earth, hectorite, kaolin, lithium magnesium silicate, lithium magnesium sodium silicate, montmorillonite, pyrophyllite, and zeolite.** *Int J Toxicol* 2003, **22(Suppl 1)**:37-102.
4. IARC: **Carbon Black and Some Nitro Compounds.** *IARC Monogr Eval Carcinog Risks Hum* 1996, **65**:149-262.
5. Hoet P, Bruske-Hohlfeld I, Salata O: **Possible health impact of nanomaterials.** In *Nanomaterials - Toxicity, health and environmental issues* Edited by: Kumar C. Weinheim: WILEY-VGH Verlag GmbH & Co. KGaA; 2006:53-80.
6. Bosi S, Da Ros T, Spalluto G, Prato M: **Fullerene derivatives: an attractive tool for biological applications.** *Eur J Med Chem* 2003, **38**:913-23.
7. IARC: **Diesel and gasoline engine exhausts and some nitroarenes.** *IARC Monogr Eval Carcinog Risks Hum* 1989, **46**:1-458.
8. Hesterberg TW, Bunn WB 3rd, Chase GR, Valberg PA, Slavin TJ, Lapin CA, Hart GA: **A critical assessment of studies on the carcinogenic potential of diesel exhaust.** *Crit Rev Toxicol* 2006, **36**:727-776.
9. Jacobsen NR, Møller P, Cohn CA, Loft S, Vogel U, Wallin H: **Diesel exhaust particles are mutagenic in FE1-MutaMouse lung epithelial cells.** *Mutat Res* 2008, **641**:54-57.
10. Hashimoto AH, Amanuma K, Hiyoshi K, Sugawara Y, Goto S, Yanagisawa R, Takano H, Masumura K, Nohmi T, Aoki Y: **Mutations in the lungs of *gpt* delta transgenic mice following inhalation of diesel exhaust.** *Environ Mol Mutagen* 2007, **48**:682-693.
11. Barrett JC, Lamb PW, Wiseman RW: **Multiple mechanisms for the carcinogenic effects of asbestos and other mineral fibers.** *Environ Health Perspect* 1989, **81**:81-89.
12. IARC: **Asbestos.** *IARC Monogr Eval Carcinog Risks Hum* 1997, **14**:11-106.
13. IARC: **Overall Evaluation of Carcinogenicity: An Updating of IARC Monographs.** *IARC Monogr Eval Carcinog Risks Hum* 1987, **1-42(suppl 7)**:106-117.
14. Baan RA: **Carcinogenic hazards from inhaled carbon black, titanium dioxide, and talc not containing asbestos or asbestiform fibers: recent evaluations by an IARC Monographs Working Group.** *Inhal Toxicol* 2007, **19(Suppl 1)**:213-228.
15. IARC: **Man-made Vitreouis Fibres.** *IARC Monogr Eval Carcinog Risks Hum* 2002, **81**:33-374.
16. Bunn WB 3rd, Bender JR, Hesterberg TW, Chase GR, Konzen JL: **Recent studies of man-made vitreous fibers. Chronic animal inhalation studies.** *J Occup Med* 1993, **35**:101-113.
17. Lam C-W, James JT, McCluskey R, Holian A, Hunter RL: **Toxicity of carbon nanotubes and its implications for occupational and environmental health.** In *Nanomaterials - Toxicity, health and environmental issues* Edited by: Kumar C. Weinheim: WILEY-VGH Verlag GmbH & Co. KGaA; 2006:130-152.
18. Donaldson K, Aitken R, Tran L, Stone V, Duffin R, Forrest G, Alexander A: **Carbon nanotubes: a review of their properties in relation to pulmonary toxicology and workplace safety.** *Toxicol Sci* 2006, **92**:5-22.
19. Poland CA, Duffin R, Kinloch I, Maynard A, Wallace WA, Seaton A, Stone V, Brown S, Macnee W, Donaldson K: **Carbon nanotubes introduced into the abdominal cavity of mice show asbestos-like pathogenicity in a pilot study.** *Nat Nanotechnol* 2008, **3**:423-428.
20. Takagi A, Hirose A, Nishimura T, Fukumori N, Ogata A, Ohashi N, Kitajima S, Kanno J: **Induction of mesothelioma in p53+/- mouse by intraperitoneal application of multi-wall carbon nanotube.** *J Toxicol Sci* 2008, **33**:105-116.
21. Nielsen GD, Roursgaard M, Jensen KA, Poulsen SS, Larsen ST: **In vivo biology and toxicology of fullerenes and their derivatives.** *Basic Clin Pharmacol Toxicol* 2008, **103**:197-208.
22. Jensen AW, Wilson SR, Schuster DI: **Biological applications of fullerenes.** *Bioorg Med Chem* 1996, **4**:767-779.
23. Nohmi T, Masumura K: **Molecular nature of intrachromosomal deletions and base substitutions induced by environmental mutagens.** *Environ Mol Mutagen* 2005, **45**:150-161.
24. Nohmi T, Suzuki M, Masumura K, Yamada M, Matsui K, Ueda O, Suzuki H, Katoh M, Ikeda H, Sofuni T: **Spi(-) selection: An efficient method to detect gamma-ray-induced deletions in transgenic mice.** *Environ Mol Mutagen* 1999, **34**:9-15.
25. Xu A, Chai Y, Hei T: **Genotoxic responses to titanium dioxide nanoparticles and fullerene in *gpt* delta transgenic MEFcells.** *Particle Fibre Toxicol* 2009, **6**:3.
26. Negishi K, Hao W: **Spectrum of mutations in single-stranded DNA phage M13mp2 exposed to sunlight: predominance of G-to-C transversion.** *Carcinogenesis* 1992, **9**:1615-1618.
27. Akasaka S, Yamamoto K: **Hydrogen peroxide induces G:C to T:A and G:C to C:G transversions in the supF gene of Escherichia coli.** *Mol Gen Genet* 1994, **243**:500-505.
28. Valentine MR, Rodriguez H, Termini J: **Mutagenesis by peroxy radical is dominated by transversions at deoxyguanosine: evidence for the lack of involvement of 8-oxo-dG1 and/or abasic site formation.** *Biochemistry* 1998, **37**:7030-7038.

29. Shin CY, Ponomareva ON, Connolly L, Turker MS: **A mouse kidney cell line with a G:C --> C:G transversion mutator phenotype.** *Mutat Res* 2002, **503**:69-76.
30. Jacobsen NR, Pojana G, White P, Møller P, Cohn CA, Korsholm KS, Vogel U, Marcomini A, Loft S, Wallin H: **Genotoxicity, cytotoxicity, and reactive oxygen species induced by single-walled carbon nanotubes andC(60) fullerenes in the FE1-Muta™ Mouse lung epithelial cells.** *Environ Mol Mutagen* 2008, **49**:476-487.
31. Valberg PA, Long CM, Sax SN: **Integrating studies on carcinogenic risk of carbon black: epidemiology, animal exposures, and mechanism of action.** *J Occup Environ Med* 2006, **48**:1291-1307.
32. Sayes CM, Marchione AA, Reed KL, Warheit DB: **Comparative pulmonary toxicity assessments of C60 water suspensions in rats: few differences in fullerene toxicity in vivo in contrast to in vitro profiles.** *Nano Lett* 2007, **7**:2399-2406.
33. Gao N, Keane MJ, Ong T, Wallace WE: **Effects of simulated pulmonary surfactant on the cytotoxicity and DNA-damaging activity of respirable quartz and kaolin.** *J Toxicol Environ Health A* 2000, **60**:153-167.
34. Kasai H, Nishimura S: **DNA damage induced by asbestos in the presence of hydrogen peroxide.** *Gann* 1984, **75**:841-844.
35. Aust A: **The role of iron in asbestos induced cancer.** In *Cellular and Molecular Effects of Mineral and Synthetic Dusts and Fibers, NATO ASI Series Volume H85*. Edited by: Davis JMG, Jaurand M-C. Berlin: Springer-Verlag; 1994:53-61.
36. Mossman BT, Gee BL: **Pulmonary reactions and mechanisms of toxicity of inhaled fibers.** In *Toxicology of the Lung* 2nd edition. Edited by: Gardner, et al. New York: Raven Press; 1993:371-387.
37. Shibutani S, Takeshita M, Grollman AP: **Insertion of specific bases during DNA synthesis past the oxidation-damaged base 8-oxodG.** *Nature* 1991, **349**:431-434.
38. Moriya M: **Single-stranded shuttle phagemid for mutagenesis studies in mammalian cells: 8-oxoguanine in DNA induces targeted G.C-->T.A transversions in simian kidney cells.** *Proc Natl Acad Sci USA* 1993, **90**:1122-1126.
39. Kornyushyna O, Berges AM, Muller JG, Burrows CJ: **In vitro nucleotide misinsertion opposite the oxidized guanosine lesions spiroiminodihydantoin and guanidinohydantoin and DNA synthesis past the lesions using Escherichia coli DNA polymerase I (Klenow fragment).** *Biochemistry* 2002, **41**:15304-15314.
40. Cadet J, Berger M, Buchko GW, Joshi PC, Raoul S, Ravanat JL: **2,2-Diamino-4-[(3,5-di-O-acetyl-2-deoxy-.beta.-D-erythro- pentofuranosyl)amino]-5-(2H)-oxazolone: a Novel and Predominant Radical Oxidation Product of 3',5'-Di-O-acetyl-2'-deoxyguanosine.** *J Am Chem Soc* 1994, **116**:7403-7404.
41. Goyal RN, Jain N, Garg DK: **Electrochemical and enzymic oxidation of guanosine and 8-hydroxyguanosine and the effects of oxidation products in mice.** *Bioelectrochemistry and Bioenergetics* 1997, **43**:105-114.
42. Ye Y, Muller JG, Luo W, Mayne CL, Shallop AJ, Jones RA, Burrows CJ: **Formation of 13C-, 15N-, and 18O-labeled guanidinohydantoin from guanosine oxidation with singlet oxygen. Implications for structure and mechanism.** *J Am Chem Soc* 2003, **125**:13926-13927.
43. Burrows CJ, Muller JG, Kornyushyna O, Luo W, Duarte V, Leipold MD, David SS: **Structure and potential mutagenicity of new hydantoin products from guanosine and 8-oxo-7,8-dihydroguanine oxidation by transition metals.** *Environ Health Perspect* 2002, **110(Suppl 5)**:713-717.
44. Kino K, Sugiyama H: **UVR-induced G-C to C-G transversions from oxidative DNA damage.** *Mutat Res* 2005, **571**:33-42.
45. Kino K, Sugiyama H: **Possible cause of G-C-->C-G transversion mutation by guanine oxidation product, imidazolone.** *Chem Biol* 2001, **8**:369-378.
46. Kino K, Ito N, Sugasawa K, Sugiyama H, Hanaoka F: **Translesion synthesis by human DNA polymerase eta across oxidative products of guanine.** *Nucleic Acids Symp Ser* 2004, **48**:171-172.
47. Hailer MK, Slade PG, Martin BD, Sugden KD: **Nei deficient Escherichia coli are sensitive to chromate and accumulate the oxidized guanine lesion spiroiminodihydantoin.** *Chem Res Toxicol* 2005, **18**:1378-1383.
48. Matter B, Malejka-Giganti D, Csallany AS, Tretyakova N: **Quantitative analysis of the oxidative DNA lesion, 2,2-diamino-4-(2-deoxy-beta-D-erythro-pentofuranosyl)amino]-5(2H)-oxazolone (oxazolone), in vitro and in vivo by isotope dilution-capillary HPLC-ESI-MS/MS.** *Nucleic Acids Res* 2006, **34**:5449-5460.
49. Justice MJ, Noveroske JK, Weber JS, Zheng B, Bradley A: **Mouse ENU mutagenesis.** *Hum Mol Genet* 1999, **8**:1955-1963.
50. Rojas E, Lopez MC, Valverde M: **Single cell gel electrophoresis: methodology and applications.** *Journal of Chromatography B* 1999, **722**:225-254.
51. Park EJ, Yoon J, Choi K, Yi J, Park K: **Induction of chronic inflammation in mice treated with titanium dioxide nanoparticles by intratracheal instillation.** *Toxicology* 2009, **260**:37-46.
52. Kaewamatawong T, Shimada A, Okajima M, Inoue H, Morita T, Inoue K, Takano H: **Acute and subacute pulmonary toxicity of low dose of ultrafine colloidal silica particles in mice after intratracheal instillation.** *Toxicol Pathol* 2006, **34**:958-65.
53. Sasaki YF, Tsuda S, Izumiyama F, Nishidate E: **Detection of chemically induced DNA lesions in multiple mouse organs (liver, lung, spleen, kidney, and bone marrow) using the alkaline single cell gel electrophoresis (Comet) assay.** *Mutat Res* 1997, **388**:33-44.
54. Toyoizumi T, Deguchi Y, Masuda S, Kinae N: **Genotoxicity and estrogenic activity of 3,3'-dinitrobisphenol A in goldfish.** *Biosci Biotechnol Biochem* 2008, **72**:2118-2123.
55. Nohmi T, Suzuki T, Masumura K: **Recent advances in the protocols of transgenic mouse mutation assays.** *Mutat Res* 2000, **455**:191-215.

Symposium date: 27th September 2009

doi:10.1093/nass/nrp106

Analysis of an RNA adduct formed from aminophenylnorharman

Koichi Nishimura[1], Yukari Totsuka[1], Takashi Higuchi[1], Nobuo Kawahara[2], Takashi Sugimura[1] and Keiji Wakabayashi[1]

[1]Cancer Prevention Basic Resarch Project, National Cancer Center Research Institute, 5-1-1 Tsukiji, Chuo-ku, Tokyo 104-0045, Japan and [2]Division of Pharmacognosy, Phytochemistry and Narcotics, National Institute of Health Sciences, 1-18-1 Kamiyoga, Setagaya-ku, Tokyo 158-8501, Japan

ABSTRACT

The endogenous mutagenic/carcinogenic 9- (4'-aminophenyl) -9*H*- pyrido [3,4-*b*] indole (aminophenylnorharman, APNH) is formed from norharman and aniline in the presence of cytochrome P-450s. The major APNH-DNA adduct has been reported to be 2'-deoxyguanosin-8-yl-aminophenylnorhaman (dG-C8-APNH). In addition, demonstrated formation of APNH-RNA adduct and conducted a structural analysis using various spectrometric approaches. The compound produced from guanosine (Guo) and *N*-acetoxy-APNH, an ultimate mutagenic form of APNH, was concluded to be guanosin-8-yl-APNH (Guo-C8-APNH) on the basis of various spectroscopic analysis. The same adduct was found in the livers of rats administered APNH. The total adduct levels of APNH-RNA were six times higher than total APNH-DNA adducts in the same rat liver samples.

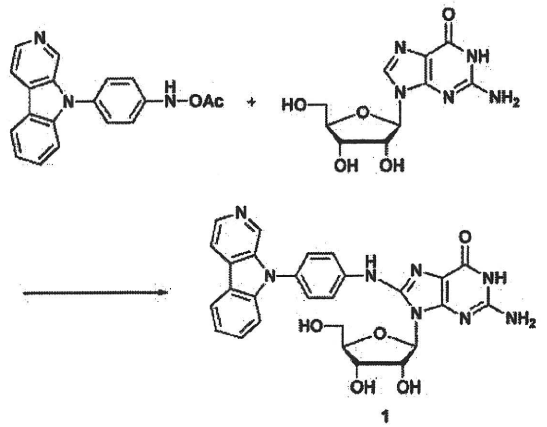

Scheme 1 A reaction mixture of *N*-acetoxy-APNH and guanosine

INTRODUCTION

Aminophenylnorharman (APNH) a product of the enzymatic reaction of norharman with aniline in the presence of S9 mix, has already been reported to be a strong mutagen/carcinogen[1-4]. Norharman and aniline abundantly exist in cigarette smoke, cooked foods and some kinds of vegetables[5-6]. Therefore, humans are exposed to both of these compounds chronically, and APNH is expected to be produced in our body. In a long term carcinogenicity experiment using experimental animals, APNH induced tumors in various tissues, including the liver and colon[3]. APNH is thought to be metabolically activated by CYP1A2 and acetyltransferase to form adducts with 2'-deoxyguanosine[7], and chemical structure of the major DNA adduct has already been reported as dG-C8-APNH, detectable in various tissues of rats and mice after a single administration of APNH[8]. In recent years, some studies have focused on RNA as a biological markers[9-11]. Similar to DNA, RNA consists of nucleobases including guanine, and would be expected to give rise to similar mutagen/carcinogen-RNA adducts. In contrast to DNA modifications by mutagens/carcinogens, which can lead to mutations, RNA modifications have generally been considered biologically meaningless. However, RNA is present in both the cytoplasmic and nuclear compartments, so it has a greater chance of reacting with the exogenous/endogenous carcinogens. Futhermore, RNA exists in a variety of forms, including tRNA, mRNA, rRNA and microRNAs, so that RNA adducts may be unique biological significance in carcinogenesis. Thus, they might offer a sensitive biomaker for exposure analysis. In the present study, we demonstrated the formation of a major APNH-RNA adduct and analyzed its chemical structure using various spectrometric approaches. In addition, we also report the generation of total APNH-RNA adducts at higher levels than total APNH-DNA lesions in the livers of rats administered APNH, as assessed by ^{32}P-postlabeling analysis[12].

RESULTS AND DISCUSSION

We first analyzed a reaction mixture of guanosine (Guo) and *N*-acetoxy-APNH (Scheme 1), an ultimate mutagenic form of APNH, by LC-ESI/MS analysis. As a result, a compound exhibiting molecular ion peak *m/z* 541 along with a fragment ion peak at *m/z* 409, consistent with loss of a ribose moiety, was found to be formed. From ^{1}H-NMR spectroscopy, its chemical structure was concluded to be guanosin-8-yl-APNH (Guo-C8-APNH) (Scheme 1). To comfirm its chemical structure, we synthesized Guo-C8-APNH via the Buchwald-Hartwig coupling reaction[13]

(Scheme 2). This product was shown to be identical to compound 1 in scheme 1 by comparison of their spectroscopic data.

Total RNA obtained from the livers of F344 rats with or without treatment of APNH was analyzed by ^{32}P-postlabeling method under adduct-intensification conditions. Adduct spot corresponding to Guo-C8-APNH were observed in the APNH-treated animals, but not in the control animals. Total adduct levels of APNH-RNA were 28±13.3 (mean±SD) adducts per 10^6 nucleotides. APNH-DNA adducts in DNA samples obtained from the same liver samples were analyzed by ^{32}P-postlabeling method under modified adduct intensification conditions. The TLC pattern was different from the case of total RNA, and their total APNH-DNA levels were 4.5±2.0 (mean±SD) adducts per 10^6 nucleotides. From these observations, it is suggested that APNH binds to both DNA and RNA *in vivo*. APNH-RNA levels were about 6 times higher than those of DNA.

CONCLUSION

We identified an APNH-RNA adduct formed by the reaction of *N*-acetoxy-APNH with Guo. The chemical structure was concluded to be Guo-C8-APNH, similar to that of dGuo-C8-APNH. Guo-C8-APNH could also be detected in rat liver after administration of APNH, suggesting that APNH can damage RNA in a manner similar to DNA *in vivo*.

We are now analyzing the function of APNH-RNA adduct using the synthesis of a Guo-C8-APNH phosphoramidite and the RNA oligonucleotide containing Guo-C8-APNH.

REFERENCES

1. Totsuka, Y., Hada, N., Matsumoto, K., Kawahara, N., Murakami, Y., Yokoyama, Y., Sugimura, T., Wakabayashi, K. (1998) *Carcinogenesis*, **19**, 1995–2000.
2. Sugimura, T. (1998) *Environ. Health Perspect.*, **106**, A522–523.
3. Kawamori, T., Totsuka, Y., Uchiya, N., Kitamura, T., Shibata, H., Sugimura, T., Wakabayashi, K. (2004) *Carcinogenesis*, **25**, 1967–1972.
4. Totsuka, Y., Takamura-Enya, T., Nishigaki, R., Sugimura, T., Wakabayashi, K. (2004) *J. Chrmatogr. B.*, **802**, 135–141.
5. Totsuka, Y., Ushiyama, H., Ishihara, J., Sinha, R., Goto, S., Sugimura, T., Wakabayashi, K. (1999) *Cancer Lett.*, **143**, 139–143.
6. Luceri, F., Pieraccini, G., Moneti, G., Dolara, P. (1993) *Toxical. Ind. Health*, **9**, 405–413.
7. Oda, Y., Totsuka, Y., Wakabayashi, K., Guengerich, F. P., Shimada, T. (2006) *Mutagenesis*, **21**, 411–16.
8. Totsuka, Y., Takamura-Enya, T., Kawahara, N., Sugimura, T., Wakabayashi, K. (2002) *Chem. Res. Toxicol.*, **15**, 1288–1294.
9. Sotomayor, R. E., Washington, M., Nguyen, L., Nyanr'anyi, R., Hinton, D. M., Chou, M. (2003) *Toxicol. Sci.*, **73**, 329-338.
10. Surh, Y. J., Lai, C. C., Miller, J. A., Miller, E. C. (1987) *Biochem. Biophys. Res. Commun.*, **144**, 576–582.
11. Zhu, P., Lee, S. H., Wehrli, S., Blair, I. A. (2006) *Chem. Res. Toxicol.*, **19**, 809–817.
12. Totsuka, Y., Nishigaki, R., Takamura-Enya, T., Kawahara, N., Sugimura, T., Wakabayashi, K. (2007) *Genes and Environment.*, **29**, 54–62.
13. Gillet, L. C., Scharer, O. D. (2002) *Org. Lett.*, **24**, 4205–4208.

*Corresponding author. E-mail: koinishi@ncc.go.jp

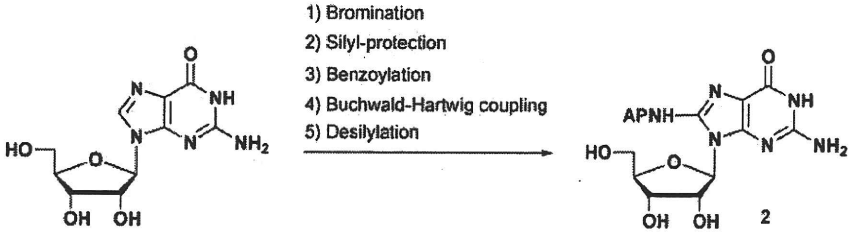

1) Br_2, water/CH_3CN; 2) DTBS(OTf)$_2$, DMF, 0 °C to r.t. 3) BnOH, PPh_3, DEAD/Dioxane; 4) APNH, Pd_2dba_3, xantphos, Cs_2CO_3, DMSO; 5) TBAF, THF

Scheme 2 Synthesis of Guo-C8-APNH

DNA AND CELL BIOLOGY
Volume 28, Number 12, 2009

Pp. 625–631
DOI: 10.1089/dna.2009.0877

Involvement of NAD(P)H:Quinone Oxidoreductase 1 and Superoxide Dismutase Polymorphisms in Ulcerative Colitis

Toshihito Kosaka,[1] Junji Yoshino,[1] Kazuo Inui,[1] Takao Wakabayashi,[1] Takashi Kobayashi,[1] Shinya Watanabe,[1] Shigekazu Hayashi,[2] Yoshifumi Hirokawa,[3] Taizo Shiraishi,[3] Takayuki Yamamoto,[4] Mayumi Tsuji,[5] Takahiko Katoh,[5] and Masatoshi Watanabe[6]

Inflammatory bowel disease is a multifactorial disease. Oxidative stress has been thought to be one of etiologic factor for inflammatory bowel disease. The genes superoxide dismutase (*SOD2*) and NAD(P)H:quinone oxidoreductase 1 (*NQO1*) are involved in inflammation and oxidative stress. The purpose of the present case–control study with 134 patients with ulcerative colitis (UC) and 125 healthy controls was to determine whether polymorphisms of these genes, the *NQO1* C609T and the *SOD2* Ala-9Val, are associated with the risk of UC and influence the clinical characteristics. These polymorphisms were examined by polymerase chain reaction–restriction fragment length polymorphisms and direct sequencing. In patients showing steroid resistance, the number with the *NQO1* T/T genotype was significantly higher than other genotypes (odds ratio 9.45, 95% confidence interval 2.46–41.6, $p = 0.002$). In the patients whose onset of UC was age 20 years or younger, more patients had *SOD2* T/T genotype than the other genotypes (odds ratio 6.46, 95% confidence interval 0.82–51.0). No association between these polymorphisms and UC risk was apparent. The *NQO1* C609T polymorphism may influence steroid resistance of UC patients, while the *SOD2* Ala-9Val polymorphism may influence age of onset of UC. Oxidative stress may influence the clinical features of UC.

Introduction

Inflammatory bowel disease (IBD) includes two common forms, Crohn's disease (CD) and ulcerative colitis (UC), and is recognized as a multifactorial disease (Koutroubakis *et al.*, 1996). Factors that may affect IBD include diet, infantile environment, and immune defense abnormalities limited to the intestinal tract. Recently, oxidative stress has been proposed to be a factor that influences IBD (Kruidenier *et al.*, 2003). Koutroubakis *et al.* (2004) showed that serum total antioxidant capacity was lower in both CD and UC patients compared with healthy controls. This finding suggests that decreased antioxidant defenses may be a primary phenomenon severely compromising the mucosa and increasing its susceptibility to oxidative tissue damage. Genetic factors have also been examined in IBD, but despite the many studies that have searched for susceptibility genes to IBD, there is currently no consensus (Orchard *et al.*, 2000). However, a recent genome-wide study for UC susceptibility genes was performed in 1052 individuals with UC (Silverberg *et al.*, 2009). In this study, UC loci attaining genome-wide significance levels were identified on chromosome 1p36 and 12q15. In this current study, we investigated the effect of NADP(H):quinone oxidoreductase 1 (NQO1) and manganese-containing superoxide dismutase (SOD2) on UC. NQO1 is an obligate two-electron reductase that catalyzes the reduction of quinines, quinine-imines, and nitro-compounds (Ross *et al.*, 2000). NQO1 may also play an antioxidant role via the reduction of endogenous quinones. The reduction of endogenous quinones helps to protect cellular membranes against oxidative damage.

SOD plays an important role in the protection of cells from the products of oxidative stress. SOD is an enzyme that catalyzes the dismutation of superoxide radicals to hydrogen

[1]Department of Internal Medicine, Second Teaching Hospital Fujita Health University School of Medicine, Nagoya, Japan.
[2]Medical Examination Center, Yachiyo Hospital, Anjou, Japan.
[3]Department of Pathologic Oncology, Mie University Graduate School of Medicine, Tsu, Japan.
[4]Inflammatory Bowel Disease Center and Department of Surgery, Yokkaichi Social Insulance Hospital, Yokkaichi, Japan.
[5]Department of Public Health, Graduate School of Medical Sciences, Kumamoto University, Kumamoto, Japan.
[6]Graduate School of Engineering, Yokohama National University, Yokohama, Japan.

peroxide. Two types of SOD lead to the requirement of the metal species at the active site: copper- and zinc-containing SOD (CuZn-SOD or SOD1, cytoplasmic) and manganese-containing SOD (Mn-SOD or SOD2, mitochondrial) (Crapo *et al.*, 1992; Guidot *et al.*, 1993). The other form is recently discovered. The forms containing Cu and Zn also have an extracellular (EC-SOD or SOD3) location (Zelko *et al.*, 2002). SOD2 is a mitochondrial enzyme that quenches free radicals and protects against oxidative stress by converting superoxide radicals to H2O2.

In this study, we conducted the study to investigate whether *NQO1* and *SOD2* polymorphisms influence the clinical characteristics of UC. In addition, the allele and genotype frequencies of the *NQO1* and *SOD2* polymorphisms were compared between UC patients and controls because of the possible influence these two polymorphisms might have on the incidence and clinical features of UC.

Materials and Methods

Subjects

We investigated 134 patients with UC (77 males and 57 females) and 125 healthy controls (67 males and 58 females). The UC patients were recruited between September 2004 and April 2007. The diagnosis of UC was based on conventional clinical, radiologic, endoscopic, and pathologic criteria. The characteristics of the UC patients are shown in Table 1. We analyzed the effect of *NQO1* and *SOD2* polymorphisms on the clinical characteristics. To assess the *NQO1* and *SOD2* polymorphisms in terms of influence on the incidence of UC, we compared the genotype frequencies of both polymorphisms in UC patients with those in controls.

Blood samples

Blood samples were collected from patients and controls after they had given informed consent to participate in this study. This study was approved by the Fujita Health University Ethics Committee. DNA was extracted from blood samples using a PUREGENE DNA isolation kit (Gentra Systems, Minneapolis, MN).

Table 1. Characteristics of Patients with Ulcerative Colitis

Age of onset (years)	36.7 ± 15.1
Colitis duration (years)	9.6 ± 7.8
Extension	
Proctitis	23 (17.2%)
Left-sided	58 (43.3%)
Pancolitis	53 (39.5%)
Type of clinical course	
First episode	16 (11.9%)
Chronic relapse	79 (59.0%)
Chronic persistent	39 (29.1%)
Severity	
Mild	40 (29.9%)
Moderate	60 (44.8%)
Severe	34 (25.3%)

The total number of patients with ulcerative colitis was 134. First episode, patients presenting with a first episode of colitis; chronic relapse, patients repeated relapse and remission; chronic persistent, patients continued active colitis over 6 months from first episode; severity is classified by Truelove and Witts' classification.

Genotypes

The *NQO1* C609T and *SOD2* Ala-9Val polymorphisms were recognized using polymerase chain reaction (PCR)–restriction fragment length polymorphisms. The primer sets were as follows (Olson *et al.*, 2004): for *NQO1*, 5′-ATTCTC TAGTGTGCCTGAG-3′ (forward) and 5′-AATCCTGCCTG GAAGTTTAG-3′ (reverse); for *SOD2*, 5′-ACCAGCAGGCA GCTGGCGCCGG-3′ (forward) and 5′-GCGTTGATGTGAG GTTCCAG-3′ (reverse). The PCR amplifications were performed in a 30-μL aliquot containing 50 ng of genomic DNA, 12 pmol of each primer, 3.0 μL of 10× buffer solution, 20 nmol/μL of dNTP, and 1 U of Taq polymerase. The PCR conditions for *NQO1* included an initial denaturation step at 95°C for 5 min, followed by 35 amplification cycles, each cycle containing denaturation at 95°C for 30 s, primer annealing at 60°C for 30 s, and extension at 72°C for 30 s, and then a final extension at 72°C for 7 min. PCR conditions for *SOD2* included an initial denaturation step at 95°C for 5 min, followed by 35 amplification cycles, each cycle containing denaturation at 95°C for 30 s, primer annealing at 63°C for 30 s, and extension at 72°C for 30 s, and then a final extension at 72°C for 7 min. The PCR products were subjected to overnight digestion with *Hin*fIV for *NQO1* at 37°C (Phillips *et al.*, 2004) and *Ngo*MIV for *SOD2* at 37°C (Akyol *et al.*, 2004) and then electrophoresed in 2% agarose gels. The digestion products gave the following band patterns: for *NQO1*, 318 bp for the wild-type C/C; 164 and 154 bp for the variant T/T; and 318, 164, and 154 bp for the heterozygous C/T (Fig. 1). For *SOD2*, the digestion products gave the following band patterns: 107 bp for the wild-type T/T; 89 and 18 bp for the variant C/C; 107, 89, and 18 bp for the heterozygous C/T (Fig. 2). Some of the digested *NQO1* and all of the *SOD2* products were examined on 12.5% polyacrylamide gels (Gene Gel Excel 12.5/24 kit from GE Healthcare Bio-Sciences, Tokyo, Japan) and stained with a DNA silver staining kit (GE Healthcare Bio-Sciences). The *NQO1* T/T genotype was expected to show two DNA bands of 164 and 154 bp; however, in this study, the T/T genotype resolved as a single band on an agarose gel. The two bands were clearly resolved on a polyacrylamide gel. The 164 and 154 bp bands showed a similar electrophoretic pattern for the C/T genotype. The band of 18 bp for the *SOD2* C/T and C/C genotypes was not clearly identified because the band was very small; however, the 107 and 89 bp bands were clearly recognized on a polyacrylamide gel. The results of PCR–restriction fragment length polymorphisms were confirmed by direct sequencing. DNA was extracted from the agarose gels using an extraction kit (Qiagen, Hilden, Germany). The genotypes were confirmed by sequence analysis using an auto sequencer (data not shown).

Statistical analysis

All data were analyzed by STATA10.0 (Stata Corporation, College Station, TX). The clinical features of UC, allele frequency, and genotype distribution were evaluated by a logistic regression test. Each polymorphism was tested to ensure that it did not deviate from Hardy–Weinberg equilibrium by the χ^2-test.